NASA Technical Paper 1595

LEVEL

Aerothermal Performance of a Radiatively and Actively Cooled Panel at Mach 6.6

Charles P. Shore and Irving Weinstein

December 1979

NASA

(18) (9)
NASA Technical Paper 1595

(19) TP-1595

(6) Aerothermal Performance of a Radiatively and Actively Cooled Panel at Mach 6.6

(10) Charles P. Shore and Irving Weinstein
Langley Research Center
Hampton, Virginia

D D C

RECEIVED

DEC 28 1979

(11) Dec 79 (12) 42

(14) NASA-LL3355

387 543

SUMMARY

A flight-weight radiative and actively cooled honeycomb sandwich panel (RACP) was subjected to multiple cycles of both radiant and aerothermal heating to evaluate its aerothermal performance. The 0.61-m (2 ft) by 1.22-m (4 ft) test specimen incorporated the essential features of a full-scale 0.61-m (2 ft) by 6.1-m (20 ft) RACP designed to withstand a uniform incident heat flux of 136 kW/m^2 (12 Btu/ft^2-sec). The test specimen consisted of René 41 heat shields backed by a thin layer of high-temperature insulation and an aluminum honeycomb sandwich panel with half-round coolant tubes next to the sandwich skin. A 60/40 mass solution of ethylene glycol/water was used to cool the RACP. A total of 15 thermal tests, five of which combined radiant and aerothermal heating segments, conducted in the Langley 8-foot high-temperature structures tunnel subjected the RACP to representative environmental heating conditions at a nominal free-stream Mach number of 6.6. The RACP successfully withstood a total of 3.5 hr of radiant heating and 137 sec in the test stream and responded to the radiant and aerothermal heating as predicted (i.e., the heat shields reached 1080 K (1945° R) and the cooled panel reached a maximum temperature of 382 K (687° R) midway between coolant tubes). Variation of the coolant inlet temperature permitted simulation of the thermal performance for the full-scale panel and indicated that the full-scale RACP would perform as expected. Post-test examination of the cooled panel revealed no evidence of coolant leakage and no evidence of hot-gas ingress which could seriously degrade the cooled-panel thermal performance.

INTRODUCTION

Actively cooled structural panels have been proposed to handle the sustained severe thermal environment which will be encountered by future hydrogen-fueled hypersonic cruise vehicles (refs. 1 to 4). Coupled to the heat sink of the liquid hydrogen fuel, active cooling allows the airframe structure to work at relatively low temperatures so that conventional materials can be used to obtain long-lived structures. Cooling of the engines and engine inlets, however, must receive top priority in design; therefore, uncertainty exists about the amount of hydrogen heat sink available for airframe cooling. It is well-known that raising the vehicle outer surface temperature to levels at which an appreciable amount of the incident heat load is radiated back to the atmosphere can substantially reduce the heat load which must be absorbed by the airframe cooling system. Thus, combining a radiative thermal protection system with an actively cooled structural panel permits adjustment of airframe cooling-system heat loads to levels compatible with hydrogen flow requirements for the engines and simultaneously allows maximum use of the available hydrogen heat-sink capacity. As discussed in reference 5, the combined radiative and actively cooled structure also reduces total system mass and provides other benefits, including increased safety and reliability, tolerance of off-design conditions, and ease of fabrication for the cooled panel.

To assess the performance characteristics of a combined radiative and actively cooled structural panel, a 0.61-m (2 ft) by 1.22-m (4 ft) test specimen was designed and fabricated under contract for tests in NASA facilities. The radiative and actively cooled test panel (described in ref. 6) incorporates all the essential features of a full-scale 0.61-m (2 ft) by 6.1-m (20 ft) panel designed to withstand a uniform incident heat flux equivalent to 136 kW/m^2 (12 Btu/ft^2-sec) to a 422 K (760° R) surface temperature. The test panel features corrugation-stiffened, beaded-skin René 41 heat shields backed by a thin layer of high-temperature insulation contained within a stainless-steel foil package and an adhesively bonded aluminum honeycomb sandwich structure with half-round coolant tubes next to the sandwich skin. Frames representative of typical transport construction support the panel at 0.61-m (2 ft) intervals. The panel was subjected to 15 thermal tests, five of which combined radiant and aerothermal heating test segments to represent environmental heating conditions. All tests were conducted in the Langley 8-foot high-temperature structures tunnel. For the aerothermal tests, the free-stream Mach number was 6.6 and the unit Reynolds number per meter was 4.7 × 10^6 (1.4 × 10^6 per foot).

Certain commercial materials are identified in this paper to specify adequately which materials were investigated in the research effort. In no case does such identification imply recommendation or endorsement of the product by NASA, nor does it imply that the materials are necessarily the only ones or the best ones available for the purpose. In many cases equivalent materials are available and would probably produce equivalent results.

SYMBOLS

Values are given in both SI Units and U.S. Customary Units. The measurements and calculations were made in U.S. Customary Units.

ℓ panel length, m (ft)

M   Mach number

p   pressure, Pa (psi)

q   dynamic pressure, Pa (psi)

$\dot{q}$ heat flux, W/m^2 (Btu/ft^2-sec)

R   unit Reynolds number, per meter (per foot)

T   temperature, K (°R)

t   time, sec

x,y   panel coordinates, cm (in.) (see fig. 5)

α angle of attack, deg (see fig. 5)

Δp differential pressure, positive inward, Pa (psi)

2

Subscripts:

l local conditions at edge of boundary layer

s   surface

t   total conditions in combustor

∞ free stream

APPARATUS AND TESTS

Radiative and Actively Cooled Panel

Design criteria.- The design of the 0.61-m (2 ft) by 1.22-m (4 ft) test panel was based on a full-scale 0.61-m (2 ft) by 6.1-m (20 ft) radiative and actively cooled panel described in detail in reference 6. To ensure that the panel was representative of hypersonic transport structure, it was designed to avoid failure from crack propagation and fatigue, to avoid catastrophic failure from loss of coolant supply, and to withstand the acoustical environment of hypersonic aircraft. The test specimen was designed to withstand a uniform incident heat flux equivalent to 136 kW/m^2 (12 Btu/ft^2-sec) to a 422 K (760° R) surface temperature. The structure was designed to sustain cyclic in-plane limit loading of ±210 kN/m (±1200 lbf/in.) parallel to the 1.22-m (4 ft) edge, and a uniform panel limit lateral pressure of ±6.89 kPa (±1.0 psi). Design life for the structure was 10 000-hr exposure to maximum temperatures and 20 000 cycles (5000 cycles with a scatter factor of four) to design limit load and temperature without fatigue failure, without crack growth to a critical length in the skins, and without surface crack growth through the thickness of the coolant passage. A factor of safety of 1.5 was applied to in-plane loads, coolant pressures, and aerodynamic pressures to obtain ultimate loads. The panel was designed for any combination of limit loads and temperature without yielding or significant permanent set and for any combination of ultimate load and temperature without failure.

General description.- The radiative and actively cooled panel (RACP) evaluated in the present investigation was designed and fabricated under contract. The test specimen consisted of five components: two heat shields, two insulation packages, and an actively cooled panel. Figure 1 shows three of the components arranged to indicate the assembly sequence. The RACP features corrugation-stiffened, beaded-skin René 41 heat shields backed by a thin layer of high-temperature insulation contained within a stainless-steel foil package and by an adhesively bonded aluminum honeycomb sandwich structure with half-round coolant tubes next to the sandwich skin. Frames representative of typical transport construction support the panel at 0.61-m (2 ft) intervals. The test panel duplicates the essential features of the full-scale design except that the coolant inlet and outlet manifolds located at the panel ends are only 1.22 m (4 ft) apart rather than 6.1 m (20 ft). The heat shield has a longitudinal row of fasteners to simulate a splice and transverse slip joints to allow thermal growth. The longitudinal splice was not necessary for the test panel

but was included since the heat-shield design does require a limited number of such splices.

Design details of heat shields and insulation packages.- Figure 2 shows some of the design details of the heat shields and insulation packages and also indicates the heat-shield support and attachment scheme. The heat shields consist of a 0.025-cm (0.010 in.) beaded outer skin and a 0.025-cm (0.010 in.) corrugated inner skin spot-welded together. Pitch of the beads and corrugations is 5.08 cm (2 in.). The crown in the beaded skin is 0.32 cm (0.125 in.); the width of the flats between beads is 2.03 cm (0.8 in.); and the height of the corrugation is 0.508 cm (0.20 in.). The insulation package consists of 256 kg/m^3 (16 lb/ft^3) Min-K insulation (manufactured by Johns-Manville Corporation) 0.32 cm (0.125 in.) thick, contained in 0.008-cm (0.003 in.) and 0.003-cm (0.001 in.) stainless-steel foil on the outer and inner surfaces, respectively. Machined stainless-steel standoff posts integrated with the insulation packages support the heat shields. Stainless-steel shoulder bolts are used to fasten the heat shields and insulation packages to the cooled panel. The bolts pass through the heat shields, standoff posts, and cooled panel and are retained by plate nuts attached to the inner skin of the cooled panel. The shoulders on the bolts provide a controlled gap to prevent clamping of the heat shields and to allow longitudinal thermal expansion of the shields. At the transverse joint, the upstream heat shield overlaps the downstream heat shield. Cutouts in the corrugations and beads allow the upstream heat shield to rest on the downstream shield all along the transverse edge. Slotted holes in the flats between corrugations are sized to accommodate thermal expansion of one-half of each shield. The shields are restrained at midspan and permitted to grow in each direction. Thermal growth in the transverse direction is absorbed by growth of the beads and corrugations.

Design details of cooled panel.- As shown in figure 3, the cooled panel is an aluminum honeycomb sandwich structure with half-round coolant tubes next to the outer skin. The coolant manifolds, tubes, and honeycomb core are adhesively bonded to the inner and outer skins of the sandwich (figs. 3(a) and 3(b)). The manifolds have dual chambers which provide uniform cooling across the panel width. Coolant enters and exits the panel at the center line through the outer manifold chamber. The manifold ends are cooled as the coolant turns the corners at the manifold ends and flows into the second chamber, where it is distributed into individual tubes. To provide close control on tube straightness and obtain bond-line thicknesses of less than 0.025 cm (0.010 in.), individual tubes were brazed to small tabs which were then bonded to small pockets machined in the manifolds (fig. 3(c)). Close control on the bond-line thickness was required to maintain the high interface conductance between the outer skin and coolant tubes that is necessary to prevent the aluminum structure from exceeding the design temperature of 422 K (760° R).

Because of cost considerations, the test-panel manifolds were fabricated as a three-piece weldment rather than an extrusion which would be used in production. To provide proper alignment of the tube/tab assemblies with the manifolds and to minimize adhesive leakage into flow passages during the bonding operation, small neoprene rods were inserted in the coolant passages through holes in the bottom of the manifolds (fig. 3(c)). After the assembly was bonded, the

4

rods were removed and the manifolds sealed with plugs. Proof pressure checks at 1.31 MPa (190 psi) and infrared scans on the completed assembly indicated the test-panel coolant flow to be reasonably uniform with no leakage.

Longitudinal and transverse splice plates 0.082-cm (0.032 in.) and 0.254-cm (0.10 in.) thick, respectively, are used to join adjacent panels and transfer loads from one panel to another in a structural assembly (fig. 3(a)). Both splice plates are mechanically fastened and adhesively bonded to the cooled panel. The adhesive provides sufficient conductivity to prevent the splice plates from exceeding the 422 K (760° R) design temperature, and since the adhesive has a low shear modulus, the fasteners were designed to transfer all the loads.

Two methods were used to provide support for the fasteners and to prevent crushing the aluminum honeycomb when installing the fasteners (fig. 3(a), section A-A). In areas under the heat-shield standoff posts where high conductivity is needed to transfer heat, an aluminum bushing was used. Away from the standoff posts, the honeycomb core was filled locally with a potting compound that cured solid when the skins were bonded to the core. Additional details of the test-panel design and fabrication are given in reference 6.

Cooling System

The system shown in figure 4 was used to cool the RACP. The system consists of a 19-kl (5000 gal) storage tank filled with a 60/40 mass solution of ethylene glycol/water, circulation pumps, flow-control valves, and a 47-kW (13.5 ton) refrigeration unit which chills the ethylene glycol mixture to 244 K (440° R). As shown in the figure 4 inset, independent pumping systems circulate the coolant from the storage tank through the test panel and refrigeration unit. To accommodate test panels with dual (redundant) flow passages, two flow loops are provided to the panel. Each loop is capable of flow rates up to 379 liter/min (100 gal/min), with independent control of coolant pressure and temperature at the test-panel inlet.

Panel Holder

Description.- The RACP was mounted in the panel holder illustrated in figure 5. Details on the development of this test fixture are given in reference 7. The panel holder has a sharp leading edge and a rectangular planform 141 cm (55.4 in.) wide by 300 cm (118 in.) long. The depth of the panel holder is 30.5 cm (12 in.). Exterior surfaces are covered with 2.54 cm (1.0 in.) thick Glasrock[1] foam tiles which protect the internal structure from the aerodynamic heating produced in the wind tunnel. The panel holder is sting mounted at its base for tests in the tunnel. Test panels are mounted in a rectangular cavity 108 cm (42.5 in.) wide by 152 cm (60 in.) long, located 102 cm (40 in.) downstream from the leading edge. Aerodynamic fences along the panel-holder sides provide two-dimensional flow over the test area, and a boundary-layer trip near

---

[1]Glasrock: Tradename of Glasrock Products, Inc.

the leading edge generates turbulent boundary-layer flow over the test-panel surface. Surface pressures and aerodynamic heating rates over the test area are varied by !tching the panel holder. Differential-pressure loading on the test panel can be controlled by regulating the cavity pressure under the test panel. Details of the differential-pressure control system are described in reference 7.

RACP installation.- Since the RACP was smaller than the test cavity in the panel holder, the closeout fixture shown in figure 6 was used to mount the RACP in the panel holder. The closeout fixture was bolted to the walls of the test cavity and consisted of 2.54-cm (1.0 in.) thick insulation blocks bonded to an aluminum-frame substructure. Some details of the RACP installation in the closeout fairing are shown in figure 7. Section A-A shows the stainless-steel forward fairing used to transition from the panel-holder surface to the RACP surface. The fixture was flush with the panel-holder surface and extended over and mated with the contour of the beaded heat shield. Insulation blocks covered with two layers of silica cloth insulation to minimize airflow into the thermal stress relief slots also provided additional support to the forward fairing. The forward fairing was fastened to the upstream wall of the test cavity with 0.24-cm (3/32 in.) diameter bolts.

Section B-B shows the interface between the longitudinal edge of the RACP and the closeout fixture. René 41 side fairings were attached to the heat shields and supported by lips on the insulation blocks and slotted L-shaped stainless-steel side retainers which were bolted to the aluminum support beams. Insulator strips isolated the side fairings from the side retainers to reduce thermal gradients in the side fairings.

The transition between the heat-shield beaded skin and the aft end of the closeout fixture is shown in section C-C of figure 7. The flats on the beaded skin of the heat shield were at the same level as the leading edge of the tapered insulation block. The flat stainless-steel aft fairing was sandwiched between the standoff posts and heat-shield skin. This arrangement left the crown portion of the beaded skin open and provided venting to relieve pressure behind the heat shield during wind-tunnel starting transients.

The RACP assembly was further secured by bolting the cooled-panel transverse support beams to the steel channel mounting beams (fig. 5), which, in turn, were bolted to the test-cavity leading- and trailing-edge walls. Metal shims were used to position the entire assembly so that the edges of the closeout fixture were flush with the panel-holder surface. In figure 8, the RACP is shown installed in the panel holder in the test chamber of the wind tunnel.

Instrumentation

The RACP was instrumented with thermocouples and pressure gages. Thermocouple locations are shown in figure 9, and pressure orifice locations are shown in figure 10. A total of 78 chromel-alumel thermocouples were used to monitor temperatures on the RACP components: 28 on the heat shields, 10 on the insulation packages, and 40 over the surfaces of the cooled panel. Surface pressures were measured at two locations, and test-cavity pressures were measured at four

6

locations under the RACP as shown in figure 10. All pressure measurements were obtained using 0.15-cm (0.06 in.) inside diameter stainless-steel orifice tubing connected to strain-gage pressure transducers located in the cavity under the RACP to avoid exposure to high temperatures. Additionally, thermocouples and pressure gages were located at the coolant inlet and outlet ports, and a turbine flow meter was located in the flow circuit to monitor these important flow parameters during the tests.

The thermocouple junctures on the heat-shield surface were formed by spot-welding the leads to the surface approximately 0.08 cm (0.03 in.) apart. On the insulation package surfaces, the thermocouple leads were spot-welded to small metal tabs which were then spot-welded to the insulation foil cover. To avoid possible crack starters from welding or peening, thermocouple junctures for the cooled panel were formed by welding the leads together to form a small bead and then bonding the thermocouples to the aluminum panel surfaces.

Besides the use of thermocouples, detailed coverage of the heat-shield surface temperatures during aerodynamic heating was obtained using an infrared radiometer system similar to that described in reference 8. The radiometer was located outside the test stream about 208 cm (82 in.) above the heat shield and scanned a 97-cm (38 in.) square as shown in figure 11. This area was surveyed by 1600 scan lines/sec and required 1/16 sec for a complete scan.

High-speed motion-picture cameras were used for photographing the RACP during wind-tunnel tests. The movie-camera locations are shown in figure 11. Still photography was used to record the RACP appearance between tests as required throughout the test series.

Test Facility

The tests were conducted in the Langley 8-foot high-temperature structures tunnel shown schematically in figure 12(a). This facility is a hypersonic blow-down wind tunnel that operates at a nominal Mach number of 7, at total pressures between 4.1 and 24.1 MPa (600 and 3500 psia), and at nominal total temperatures between 1390 and 2000 K (2500° and 3600° R). Corresponding free-stream Reynolds numbers are between 1×10^6 and 10×10^6 per meter (0.3×10^6 and 3.0×10^6 per foot). Within the operating envelope bounded by these conditions, the aerodynamic pressures and heating rates encountered in flight at Mach 7 in the altitude range between 24 and 40 km (80 000 and 130 000 ft) are obtained. Other details on this test facility are reported in reference 7.

The test model is initially stored in a pod below the test stream (fig. 12(b)) to protect it from adverse tunnel start-up transients and acoustic loads. The model is covered with acoustic baffles (figs. 12(b) and 12(c)) until the desired hypersonic flow conditions are established. The baffles are then retracted and the model rapidly inserted into the stream on a hydraulically actuated elevator capable of traveling the 2.1 m (7 ft) to the center of the stream in approximately 1 sec. A model pitch system provides a range of angles of attack of -20° to 20°. Before tunnel shutdown, the model is withdrawn from the stream and covered with the acoustic baffles. The baffles attenuate the

7

acoustic energy from approximately 8 to 12 dB over the range of combustor pressure. Other details of the acoustic baffles are given in reference 7.

A heater system was used for both the static radiant tests and as a pre-heater for the aerothermal tests. The heater system consisted of quartz-lamp radiators mounted inside the acoustic-baffle boxes (fig. 12(b)). The radiant lamps were powered by an ignitron tube power supply and were controlled by a closed-loop servo system to give the desired temperature histories. Surface temperatures above 1255 K (2260° R) can be obtained using the preheat system. A more detailed discussion of the preheat system is given in reference 7.

Tests

To assess the thermal and aerothermal performance of the RACP, it was subjected to repeated radiant heating thermal tests and radiant-preheat aero-thermal tests (designated aerothermal tests), with temperature histories similar to those shown in figure 13. For both the radiant heating thermal and aerothermal tests, the coolant flow circulation system was started and the system adjusted until the desired values for coolant inlet temperature and pressure and flow rate were obtained. The radiant lamps were then used to heat the RACP at 2.8 K/sec (5° R/sec) until the heat shields reached approximately 1060 K (1910° R). For the radiant heating thermal tests (fig. 13(a)), the heat-shield temperature was held at approximately 1060 K (1910° R) for periods of 80 to 5016 sec to allow the RACP to reach thermal equilibrium; to terminate a test, the surface was allowed to cool at 2.8 K/sec (5° R/sec) until natural cooling occurred at a lower rate. For the aerothermal test (fig. 13(b)), the heat-shield temperature was held at approximately 1060 K (1910° R) until the RACP reached thermal equilibrium. The tunnel was then started and after flow was established (note change in time scale), the heat-ers were retracted and the RACP injected into the stream. About 15 sec elapsed from the time the heaters were retracted until the RACP entered the stream and was pitched to the desired angle of attack. During this process, the heat shields cooled to about 950 K (1710° R). Aerodynamic heating pro-vided by the stream rapidly reheated the heat shields to about 1090 K (1960° R). However, because of the short run time and lag in thermal response of the cooled panel provided by the insulation, the cooled panel did not recover to its ini-tial equilibrium temperature. At the end of the tunnel run, the RACP was retracted from the stream and covered by the lamps and acoustic baffles, the tunnel was shut down, and the heaters were used to control the RACP cooling rate.

Data Acquisition

During thermal tests and preheating for tunnel tests, thermocouple and strain-gage outputs were recorded at 2-sec intervals. During the aerothermal portion of the tests, thermocouple and pressure-transducer outputs were recorded at a sampling rate of 20/sec. Analytical quantities reported herein for the wind-tunnel tests are based on the thermal, transport, and flow proper-ties of the combustion products test medium as determined from reference 9. Results from tunnel-stream survey tests (ref. 10) were used to determine free-

8

stream conditions in the test section from reference measurements in the combustion chamber. Local Mach number and flow conditions were obtained from oblique-shock relations.

RESULTS AND DISCUSSION

Summary of Panel Tests

The RACP was subjected to a total of 15 thermal cycles; of these, 10 were radiantly heated thermal tests and 5 were aerothermal tests with radiant preheat. A test summary is given in table I. The order of testing, nominal heat-shield surface temperature, time at peak surface temperature, coolant inlet and outlet temperature, nominal coolant flow rate, and absorbed heat flux are included in the table. All the tests were conducted at a nominal coolant flow rate of 13 ℓ/min (3.4 gal/min). In the tests, the nominal heat-shield surface temperature ranged from 1012 K (1821° R) to 1103 K (1986° R), and the coolant inlet temperature was varied from 279 K (502° R) to 333 K (600° R). During the test program, the RACP was exposed to elevated heat-shield temperatures for 3.5 hr and to the Mach 6.6 stream for 137 sec. Figure 14 contains a summary of the nominal heat-shield surface temperature and coolant inlet temperature histories for each test. Free-stream and local aerothermal test conditions, differential pressure across the RACP, unit Reynolds number, and calculated incident cold-wall heat flux are summarized in table II. These tests imposed inward acting differential pressures of approximately 2 kPa (0.3 psi) and a nominal heat flux of 136 kW/m^2 (12 Btu/ft^2-sec) on the RACP.

RACP Thermal and Aerothermal Performance

Typical longitudinal temperature distributions from both radiant and aerothermal heating of the RACP (test 14) are shown in figure 15. The measured temperatures are compared with analytical temperatures presented in reference 6. The predicted temperatures for the heat shields are for the flats between the beads and the bottom of the corrugations. The predicted temperatures for the cooled panel are for the outer skin midway between the coolant tubes and for regions adjacent to fasteners which penetrate the cooled panel. Both the radiant and aerothermal heating of the RACP produce similar results, except that the time of exposure in the wind tunnel was not sufficient to bring the cooled panel back to equilibrium temperatures. The good agreement between the measured and analytical temperatures indicates that the RACP performed as expected, and the good agreement between the radiant and aerothermal heating results indicates that the slip joint between the heat shields prevented hot-gas ingress to the cooled panel which could seriously degrade the RACP thermal performance. The mismatch between temperatures on the insulation inner surface and the cooled panel probably results from a gap between the insulation and panel caused by instrumentation leads. In fact, the problem appears to worsen near the outlet end of the panel where the number of instrumentation leads is largest.

A temperature distribution through an RACP cross section is shown in figure 16 (test 14 radiant preheat). This figure indicates that the major temperature drop from the heat-shield temperature of 1065 K (1918° R) to the

9

cooled-panel surface temperature of 370 K (667° R) occurs across the 0.32-cm (0.125 in.) thick insulation layer. The figure also shows that the inner skin of the cooled panel is operating about 18 K (32° R) cooler than the outer surface. Analytical predictions in reference 6 indicate only about a 5 K (10° R) temperature difference between the inner and outer cooled-panel surfaces. However, the results in reference 6 were obtained for an adiabatic (no heat loss) inner surface. In reality, the inner skin loses some heat to its surroundings and the 18 K (32° R) temperature difference is not considered excessive.

A temperature contour plot from the infrared scanner is shown in figure 17 for the forward heat shield (test 15). The figure indicates that the heat-shield fasteners reach temperatures that are at least 25 K (45° R) hotter than surrounding areas of the heat shields. Similar results were obtained for some heat-shield tests reported in reference 11. Many of the exposed fasteners penetrate the cooled panel and thus provide a direct heat path ("heat short") to the interior of the cooled panel. The design of the RACP included the effects of such heat shorts; however, the short duration of the aerothermal tests prevented experimental assessment of the heat short problem.

Full-Scale Panel Simulation

One of the objectives of the RACP test program was to simulate the thermal performance of a full-scale 0.61-m (2 ft) by 6.1-m (20 ft) radiative and actively cooled panel. However, the 1.22-m (4 ft) test panel differs from the full-scale panel in two major respects: the insulation layer thickness is 0.32 cm (0.125 in.) rather than 0.38 cm (0.15 in.), and the panel length is 1.22 m (4 ft) rather than 6.1 m (20 ft). For the same temperatures in the test panel and the full-scale panel, the effect of the thinner insulation is to allow more heat to penetrate through to the cooled panel so that the cooled test panel must absorb 10.9 kW/m^2 (0.96 Btu/ft^2-sec) rather than the design value of 9.1 kW/m^2 (0.8 Btu/ft^2-sec). Since the heat-transfer coefficient inside the coolant tubes, however, is inversely proportional to the panel length (ref. 6), the heat-transfer coefficients in the test panel are larger than those in the full-scale panel; therefore, the test panel absorbs heat more efficiently than the full-scale panel.

The thinner insulation and larger heat-transfer coefficients have opposite effects on the test-panel performance compared with the full-scale panel performance. The thinner insulation requires a larger test-panel coolant temperature rise than for the full-scale panel. The larger heat-transfer coefficients for the test panel result in a lower test-panel coolant temperature rise than for the full-scale panel. Although the two effects partially offset each other, the effect of the larger heat-transfer coefficients for the test panel is much greater than the effect of the thinner insulation. Thus, to properly simulate cooled-panel temperature for the full-scale panel, it was necessary to vary the test-panel coolant inlet temperature. Figure 18 shows test-panel temperature response as a function of coolant inlet temperature. The coolant outlet temperature and the temperature along the panel center line midway between cooling tubes at two locations (one 15.2 cm (6 in.) from the coolant inlet and the other 15.2 cm (6 in.) from the coolant outlet) are shown. Analytical predictions from reference 6 are shown for comparison. The measured and predicted

10

temperatures agree very well and indicate that by varying the coolant inlet temperature from 283 K (510° R) to 333 K (600° R), cooled-panel temperatures ranging from 323 K (582° R) to 384 K (692° R) can be obtained.

Simulated full-scale cooled-panel temperatures are compared with analytical predictions from reference 6 in figure 19, where RACP center-line temperatures midway between coolant tubes are shown as a function of panel length. The predicted test-panel coolant temperature curve was obtained by adjusting the temperature difference between the predicted full-scale cooled-panel temperature and the predicted full-scale coolant temperature by the ratio of the heat-transfer coefficient in the full-scale panel to the heat-transfer coefficient in the test panel. The test data were plotted by locating the coolant inlet temperature on the predicted test-panel coolant temperature curve and then plotting cooled-panel temperatures and coolant outlet temperature as a function of test-panel length from that point. To eliminate flow entry and heat short effects, only cooled-panel temperatures in the last 0.6 m (2 ft) of the test panel away from fasteners are shown. Both the coolant and cooled-panel measured temperatures agree very well with analytical predictions. The good agreement between measured and predicted temperatures indicates that the 1.22-m (4 ft) test panel can be used to simulate the thermal performance of the 6.1-m (20 ft) full-scale RACP and that the full-scale RACP can be expected to meet its thermal performance design goals.

RACP Posttest Condition

Except for some slight discoloration over the heat-shield surfaces and oxidation on the stainless-steel foil enclosing the insulation, the RACP was in excellent condition at the conclusion of the test series. Figure 20 shows the posttest condition of the heat shields. The light-shaded rub marks at the center slip joint indicate that the heat shields moved about 0.6 cm (0.25 in.) when heated to test temperatures. This value is consistent with calculated values for the 790 K (1420° R) temperature change from ambient conditions. Additionally, there was no evidence of binding at the joints or buckling of the heat-shield skins.

The RACP was easily disassembled after the test series for visual inspection of the insulation packages and the outer surface of the cooled panel. The inspection revealed no evidence of failure of any component parts. The posttest condition of the insulation packages is shown in figure 21. The stainless-steel foil covering for the insulation next to the hot heat-shield surface showed some mild oxidation, but the insulation package remained completely intact and showed no other signs of deterioration. The appearance of the cooled panel after the test series was virtually unchanged, and there were no signs of either hot-gas ingress to the cooled-panel outer surface or coolant leakage as a result of the tests.

CONCLUDING REMARKS

A flight-weight radiative and actively cooled honeycomb sandwich structural panel (RACP) applicable to hydrogen-fueled hypersonic aircraft was

11

subjected to multiple cycles of both radiant and aerothermal heating to evaluate its aerothermal performance. The 0.61-m (2 ft) by 1.22-m (4 ft) test specimen was designed and fabricated under contract for tests in NASA facilities. The test panel incorporated all the essential features of a full-scale 0.61-m (2 ft) by 6.1-m (20 ft) radiative and actively cooled panel designed to withstand a uniform incident heat flux equivalent to 136 kW/m^2 (12 Btu/ft^2-sec) to a 422 K (760° R) surface temperature. The test specimen featured corrugation-stiffened, beaded-skin René 41 heat shields backed by a thin layer of high-temperature insulation contained within a stainless-steel foil package and an adhesively bonded aluminum honeycomb sandwich structure with half-round coolant tubes next to the sandwich skin. A 60/40 mass solution of ethylene glycol/water was used to cool the RACP. Frames representative of typical transport aircraft construction supported the panel at 0.61-m (2 ft) intervals. The RACP was subjected to 15 thermal tests, five of which combined radiant and aerothermal test segments to represent environmental heating conditions. All aerothermal tests were conducted in the Langley 8-foot high-temperature structures tunnel at a nominal free-stream Mach number of 6.6. The RACP was heated by radiant lamps for a total of 3.5 hr at a surface temperature of approximately 1060 K (1910° R) and was tested in the stream for a total of 137 sec.

The tests revealed that the RACP responded to radiant and aerothermal heating as predicted: the heat shields reached 1080 K (1945° R), the cooled panel reached a maximum temperature of 382 K (687° R) midway between coolant tubes, and the cooled-panel absorbed heat flux ranged from 9.4 kW/m^2 (0.83 Btu/ft^2-sec) to 11.9 kW/m^2 (1.05 Btu/ft^2-sec). Variation of the test-panel coolant inlet temperature permitted simulation of the thermal performance for the full-scale 0.61-m (2 ft) by 6.1-m (20 ft) radiative and actively cooled panel and indicated that the full-scale RACP can be expected to meet its thermal performance design goals. Posttest examination of the cooled panel revealed no evidence of either coolant leakage or hot-gas ingress to the cooled panel which could seriously degrade its thermal performance.

Langley Research Center
National Aeronautics and Space Administration
Hampton, VA 23665
November 20, 1979

12

REFERENCES

1. Becker, John V.: New Approaches to Hypersonic Aircraft. Paper presented at the Seventh Congress of the International Council of the Aeronautical Sciences (Rome, Italy), Sept. 1970.

2. Helenbrook, R. G.; and Anthony, F. M.: Design of a Convective Cooling System for a Mach 6 Hypersonic Transport Airframe. NASA CR-1918, 1971.

3. Anthony, F. M.; Dukes, W. H.; and Helenbrook, R. G.: Internal Convective Cooling Systems for Hypersonic Aircraft. NASA CR-2480, 1975.

4. Pirrello, C. J.; Baker, A. H.; and Stone, J. E.: A Fuselage/Tank Structure Study for Actively Cooled Hypersonic Cruise Vehicles – Summary. NASA CR-2651, 1976.

5. Kelly, H. Neale; Wieting, Allan R.; Shore, Charles P.; and Nowak, Robert J.: Recent Advances in Convectively Cooled Engine and Airframe Structures for Hypersonic Flight. NASA CP-2065, Part I, Recent Advances in Structures for Hypersonic Flight, 1978, pp. 47-61.

6. Ellis, D. A.; Pagel, L. L.; and Schaffer, D. M.: Design and Fabrication of a Radiative Actively Cooled Honeycomb Sandwich Structural Panel for a Hypersonic Aircraft. NASA CR-2957, 1978.

7. Deveikis, William D.; Bruce, Walter E., Jr.; and Karns, John R.: Techniques for Aerothermal Tests of Large, Flightweight Thermal Protection Panels in a Mach 7 Wind Tunnel. NASA TM X-71983, 1974.

8. Boylan, D. E.; Carver, D. B.; Stallings, D. W.; and Trimmer, L. L.: Measurement and Mapping of Aerodynamic Heating Using a Remote Infrared Scanning Camera in Continuous Flow Tunnels. A Collection of Technical Papers – AIAA 10th Aerodynamic Testing Conference, Apr. 1978, pp. 213-231. (Available as AIAA Paper No. 78-799.)

9. Leyhe, E. W.; and Howell, R. R.: Calculation Procedure for Thermodynamic, Transport, and Flow Properties of the Combustion Products of a Hydrocarbon Fuel Mixture Burned in Air With Results for Ethylene-Air and Methane-Air Mixtures. NASA TN D-914, 1962.

10. Deveikis, William D.; and Hunt, L. Roane: Loading and Heating of a Large Flat Plate at Mach 7 in the Langley 8-Foot High-Temperature Structures Tunnel. NASA TN D-7275, 1973.

11. Deveikis, William D.; Miserentino, Robert; Weinstein, Irving; and Shideler, John L.: Aerothermal Performance and Structural Integrity of a René 41 Thermal Protection System at Mach 6.6. NASA TN D-7943, 1975.
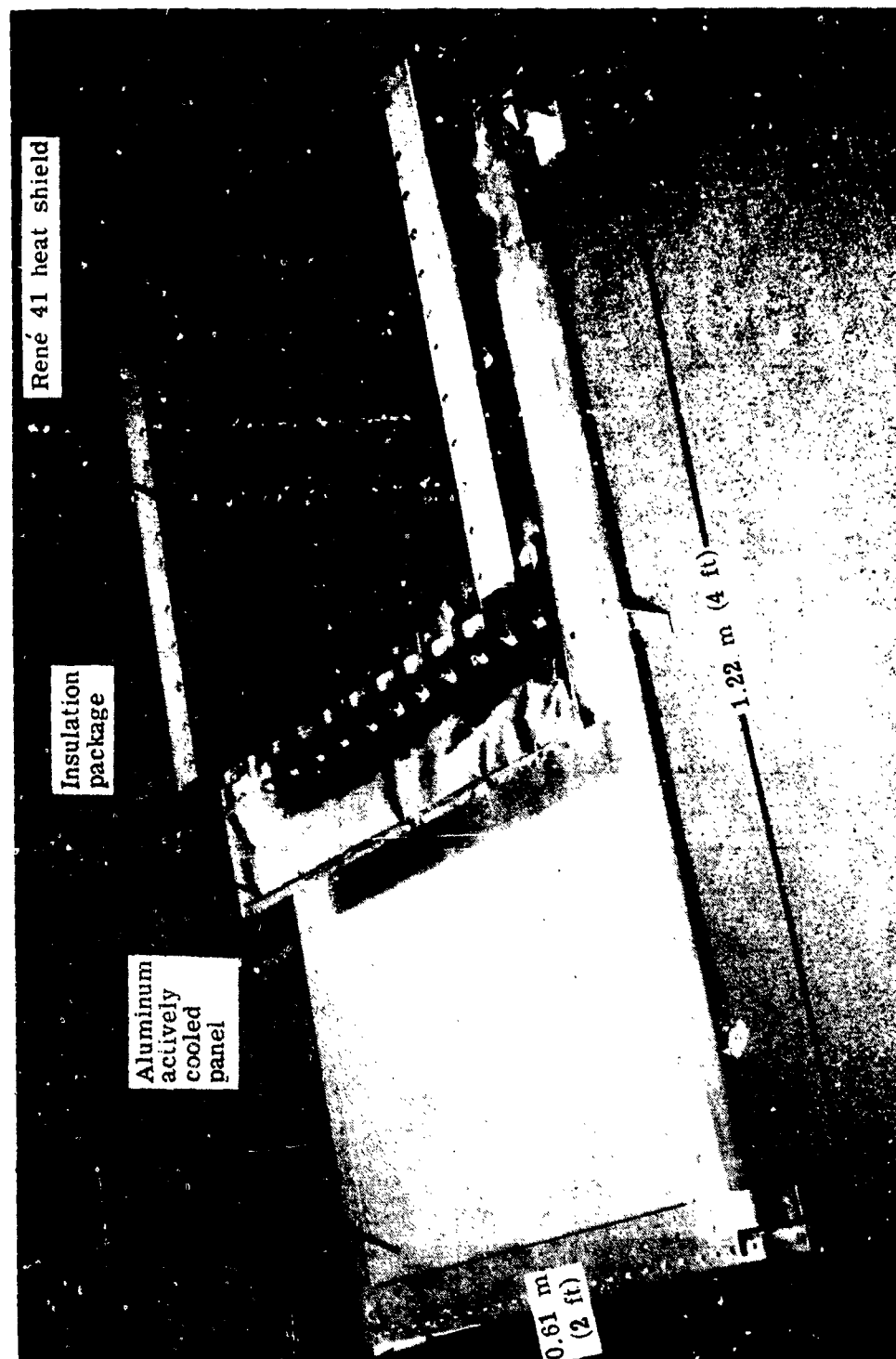
TABLE I.- TEST SUMMARY

Test	Type of test	Nominal heat-shield surface temperature		Time at peak surface temperature, sec		Coolant temperature				Nominal flow rate		Absorbed heat flux	
						Inlet		Outlet					
		K	°R	Radiant	Aerothermal	K	°R	K	°R	ℓ/min	gal/min	kW/m²	Btu/ft²-sec
1	Radiant	1066	1919	110	-----	298	537	309	556	13.0	3.4	9.41	0.83
2	Radiant	1065	1917	80	-----	298	537	309	556	13.0	3.4	9.41	.83
3	Radiant	1024	1844	270	-----	295	530	306	551	13.0	3.4	10.09	.89
4	Radiant	1012	1821	300	-----	300	540	311	559	13.0	3.4	9.97	.88
5	Radiant	1044	1880	280	-----	287	517	298	536	13.0	3.4	9.97	.88
6	Aerothermal	1033	1860	585	8.5	285	513	299	538	13.0	3.4	10.65	.94
7	Radiant	1050	1890	535	-----	283	510	295	531	13.0	3.4	10.09	.89
8	Radiant	1081	1945	1 155	-----	283	510	295	533	13.0	3.4	10.88	.96
9	Aerothermal	1066	1919	610	30.2	279	502	291	524	13.4	3.5	11.33	1.00
10	Aerothermal	1066	1919	950	30.3	290	523	303	545	12.6	3.3	11.45	1.01
11	Radiant	1070	1926	550	-----	333	600	344	620	13.4	3.5	10.88	.96
12	Radiant	1070	1926	5 016	-----	324	584	337	606	11.9	3.1	10.20	.90
13	Radiant	1071	1927	550	-----	321	578	333	599	13.0	3.4	11.33	1.00
14	Aerothermal	1080	1944	805	30.0	327	588	339	610	13.0	3.4	11.33	1.00
15	Aerothermal	1103	1986	800	37.5	303	546	317	570	13.0	3.4	11.90	1.05
	Total time			12 596	136.5								

14

TABLE II.- AEROTHERMAL TEST CONDITIONS

Test	α, deg	T_t, K (°R)	P_c, MPa (psia)	P_∞, kPa (psia)	q_∞, kPa (psia)	M_∞	M_l	P_l, kPa (psia)	q_l, kPa (psia)	Δp_s, kPa (psi)	R_∞, per meter (per foot)	$\dot{q}$, kW/m² (Btu/ft²-sec)
6	8.2	1700	17.06	2.110	61.43	6.48	5.18	6.76	125.48	+2.34	4.86×10^6	131.76
		(3060)	(2475)	(0.306)	(8.91)			(0.98)	(18.20)	(+0.34)	(1.48×10^6)	(11.61)
9	8.0	1767	17.00	2.075	62.67	6.60	5.26	6.62	127.00	+2.41	4.72×10^6	132.44
		(3180)	(2465)	(0.301)	(9.09)			(0.96)	(18.42)	(+0.35)	(1.44×10^6)	(11.67)
10	8.0	1850	17.06	2.013	60.05	6.73	5.32	6.41	124.93	+2.55	4.43×10^6	137.44
		(3330)	(2475)	(0.292)	(8.71)			(0.93)	(18.12)	(+0.37)	(1.35×10^6)	(12.11)
14	8.0	1781	17.34	2.103	65.02	6.62	5.26	6.83	130.86	+2.21	4.86×10^6	136.41
		(3205)	(2515)	(0.305)	(9.43)			(0.99)	(18.98)	(+0.32)	(1.48×10^6)	(12.02)
15	8.3	1872	17.00	1.979	61.36	6.78	5.36	6.27	119.62	+2.07	4.43×10^6	142.54
		(3370)	(2465)	(0.287)	(8.90)			(0.91)	(17.35)	(+0.30)	(1.35×10^6)	(12.56)

Figure 1.- Radiative and actively cooled test panel.

René 41 heat shield

Insulation package

Aluminum actively cooled panel

1.22 m (4 ft)

0.61 m (2 ft)

L-79-352

0.0254 (0.010)

0.0254 (0.010)

René 41 heat shield

Beaded skin

Corrugated skin

5.08 (2.0)

1.83 (0.72)

3.05 (1.20)

0.508 (0.20)

0.87 (0.345)

Standoff post

Stainless foil

Insulation

Stainless foil 0.008 (0.003)

0.003 (0.001) stainless foil

0.318 (0.125)

Standoff post

Attachment detail

Heat-shield joint
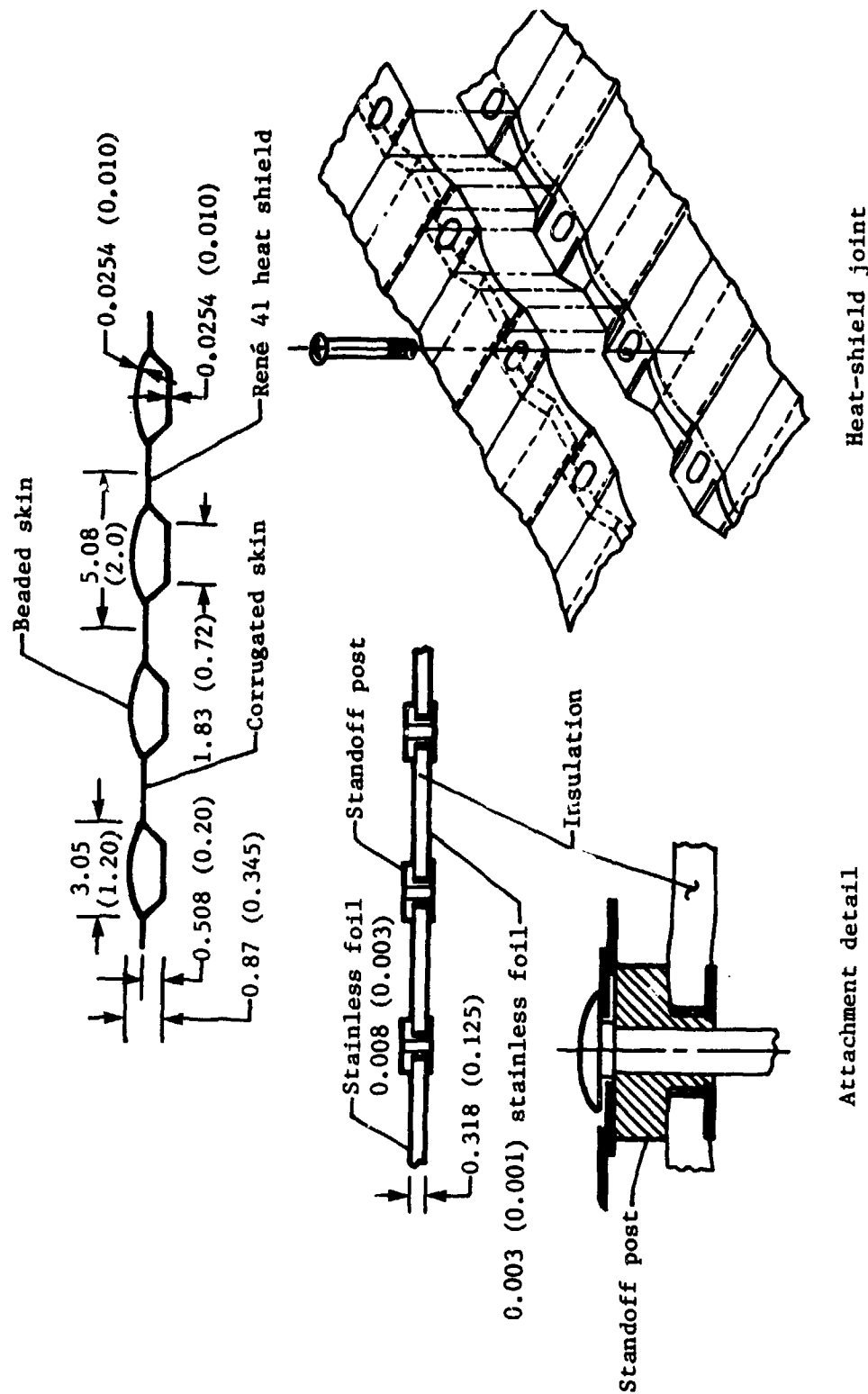
Figure 2.- Heat shield and insulation details. (Dimensions are in cm (in.).)

17

Frame

Longitudinal
splice

Polysulfide
sealant

D-shaped
coolant
tubes

Honeycomb

Skins

Manifold

Transverse splice

Bulkhead

Plate nut

Asbestos phenolic

Potting compound

High-strength fastener

A-A

Aluminum bushing
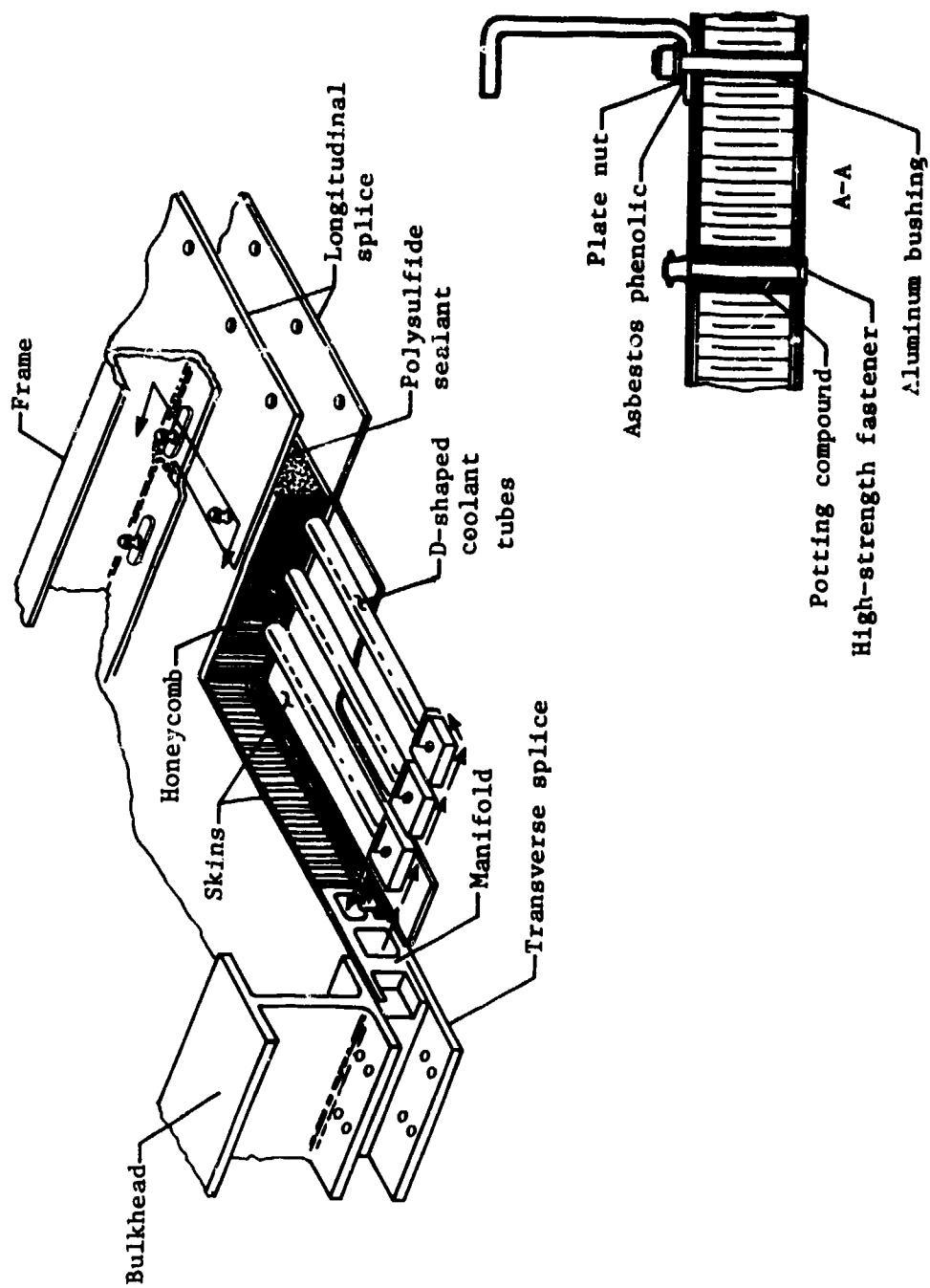
(a) Assembly.

Figure 3.- Actively cooled panel details.

18

Honeycomb core

2.54 (1.00)

0.101 (0.040)

0.101 (0.040)

3.01 (1.185)

Cooled panel

0.51 (0.201)

2.76 (1.087)

0.204 (0.080)

0.51 (0.20)

0.204 (0.080)

1.58 (0.625)

2.80 (1.105)

2.12 (0.835)

0.204 (0.080)

3.36 (1.325)

6.66 (2.625)

0.204 (0.080)

0.204 (0.080)

2 63 (1.034)

0.204 (0.080)

Manifold

0.0762 (0.030)

0.276 (0.105)

0.204 (0.080)

0.051 (0.020)

0.576 (0.227)

Tube

(b) Panel geometry.

Figure 3.- Continued.

Film adhesive

Brazed
tube/tab
assembly

Film adhesive

Manifold

A

A

(c) Tube-manifold attachment.

Figure 3.- Concluded.

Outer skin

Tube

Tab

Plug

Section A-A

20

FLOW CONTROL VALVES

COOLANT STORAGE TANK

CIRCULATION PUMP
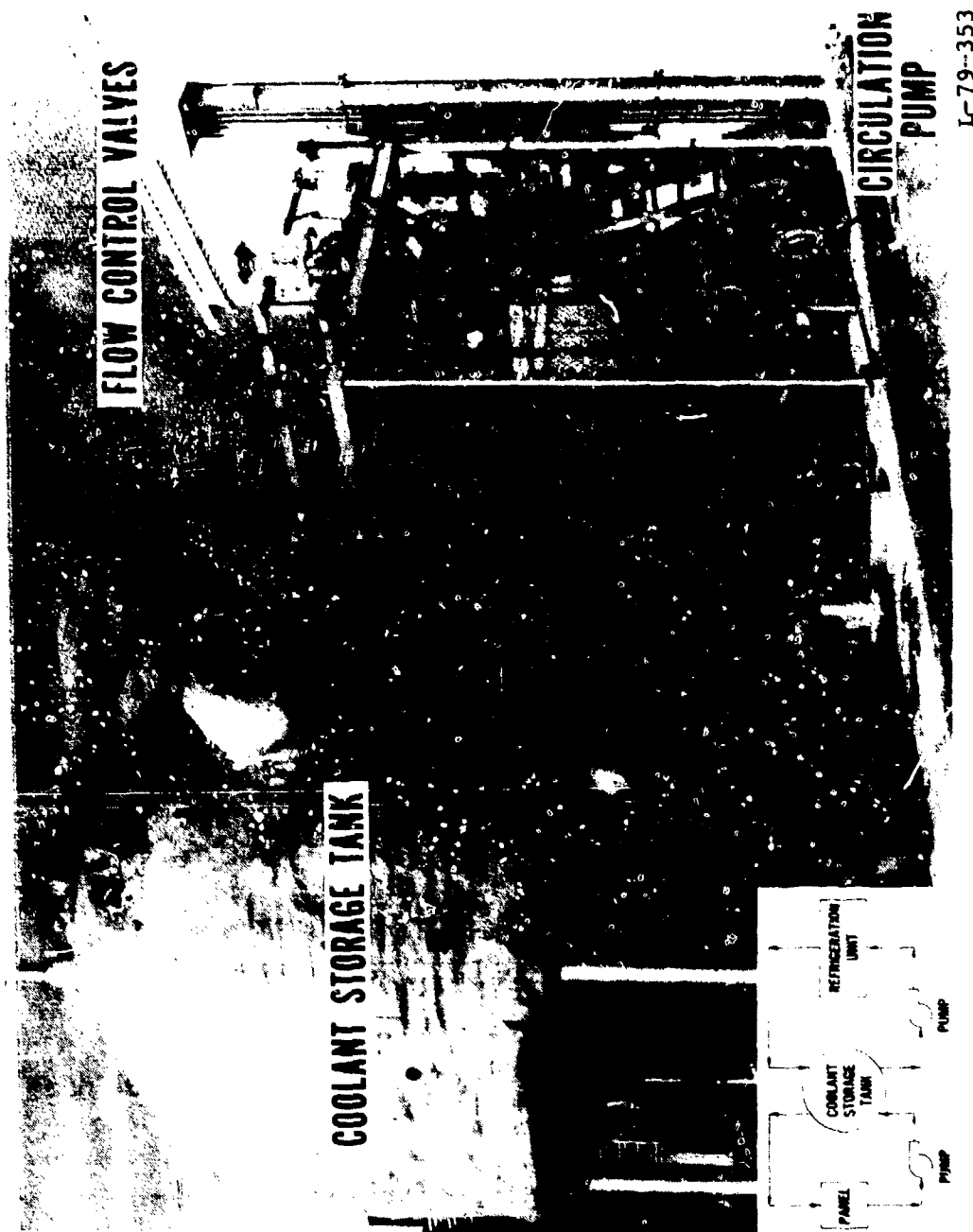
L-79-353

Figure 4.- Test-panel cooling system.

21
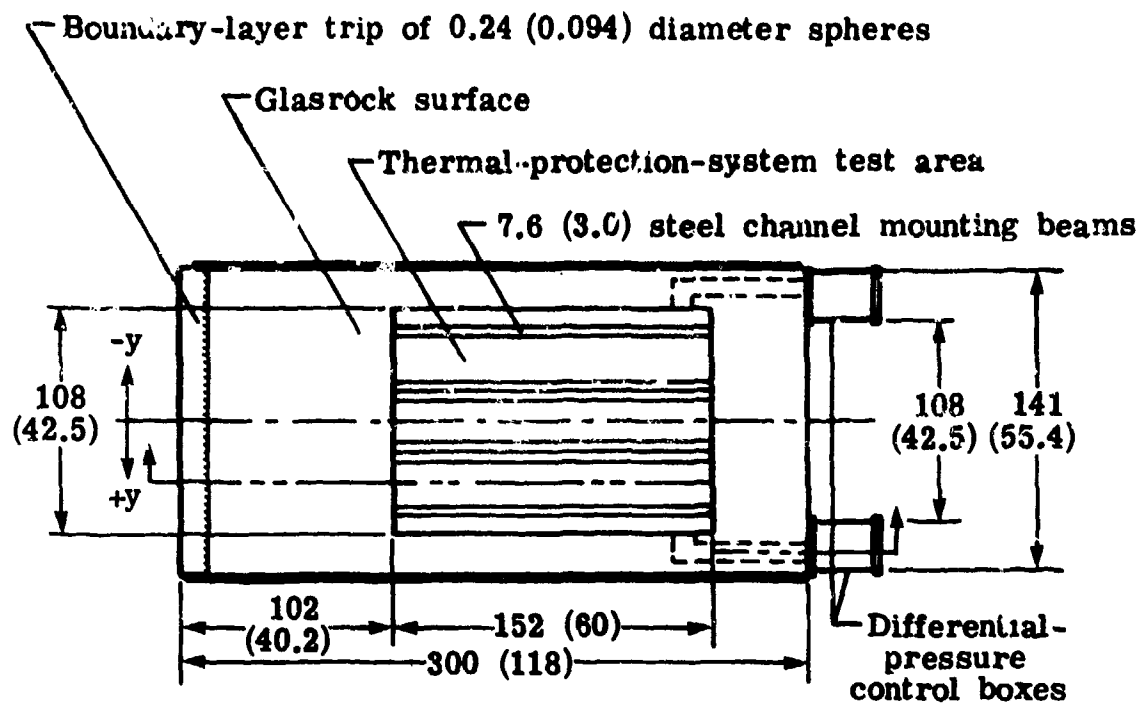
(a) Planview without test panel.
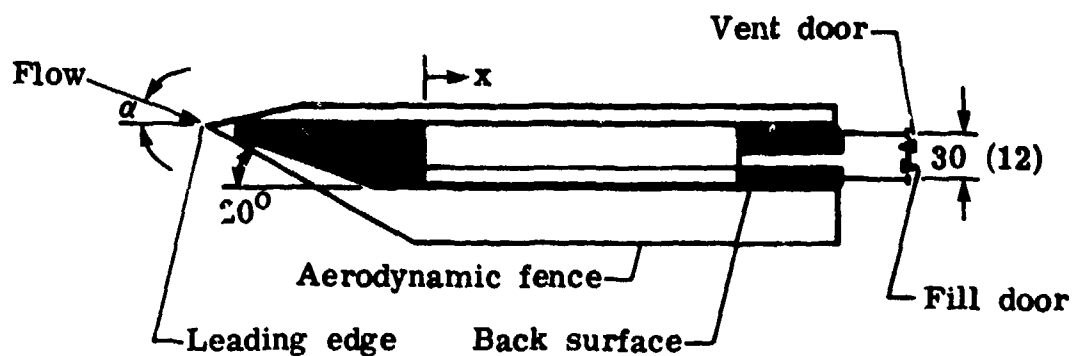
(b) Longitudinal cross section.

Figure 5.- Details of panel holder. (Dimensions are in cm (in.).)

22

SIDE FAIRINGS

FORWARD FAIRING
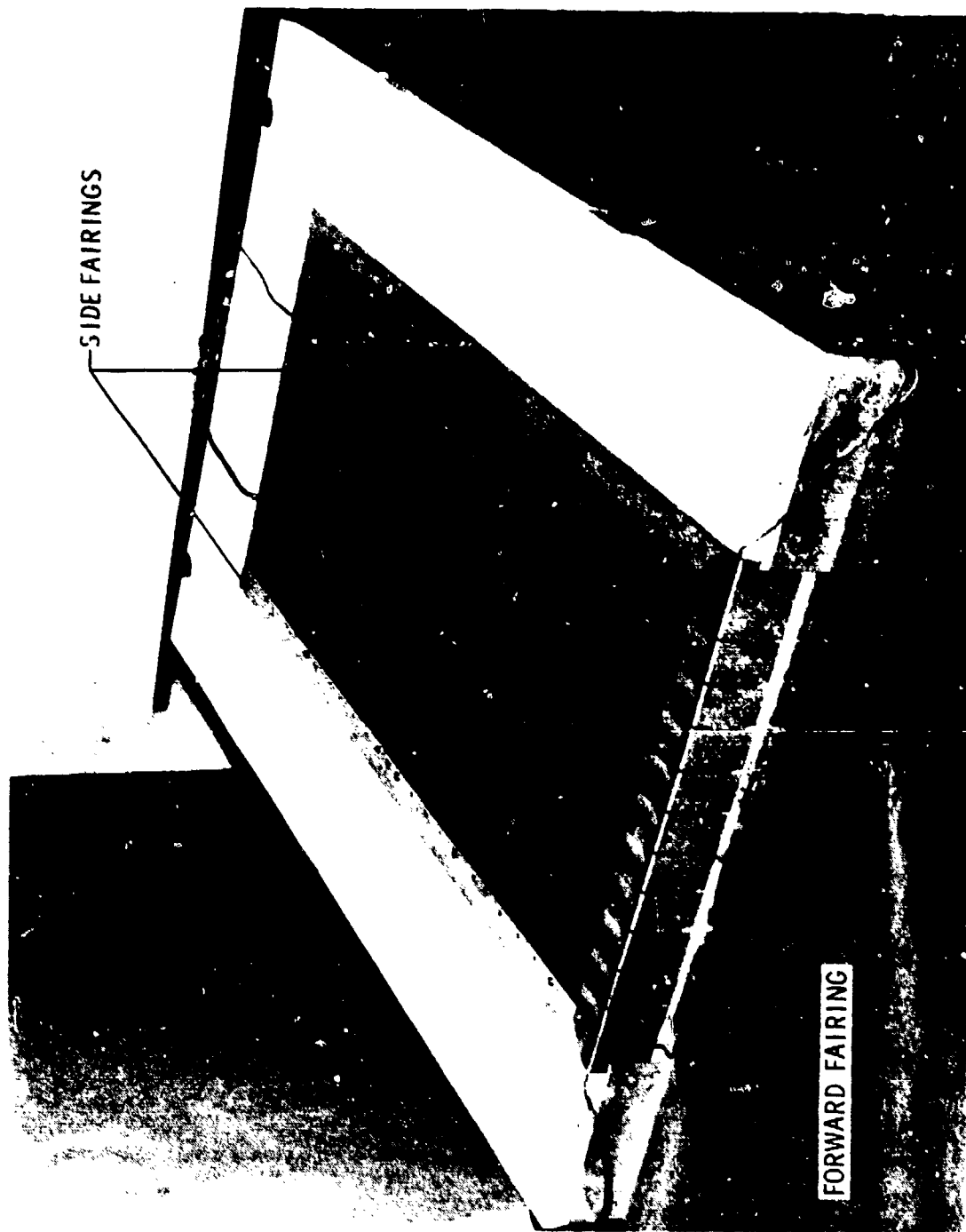
Figure 6.- Test panel mounted in wind-tunnel closeout fixture.

L-79-354

23
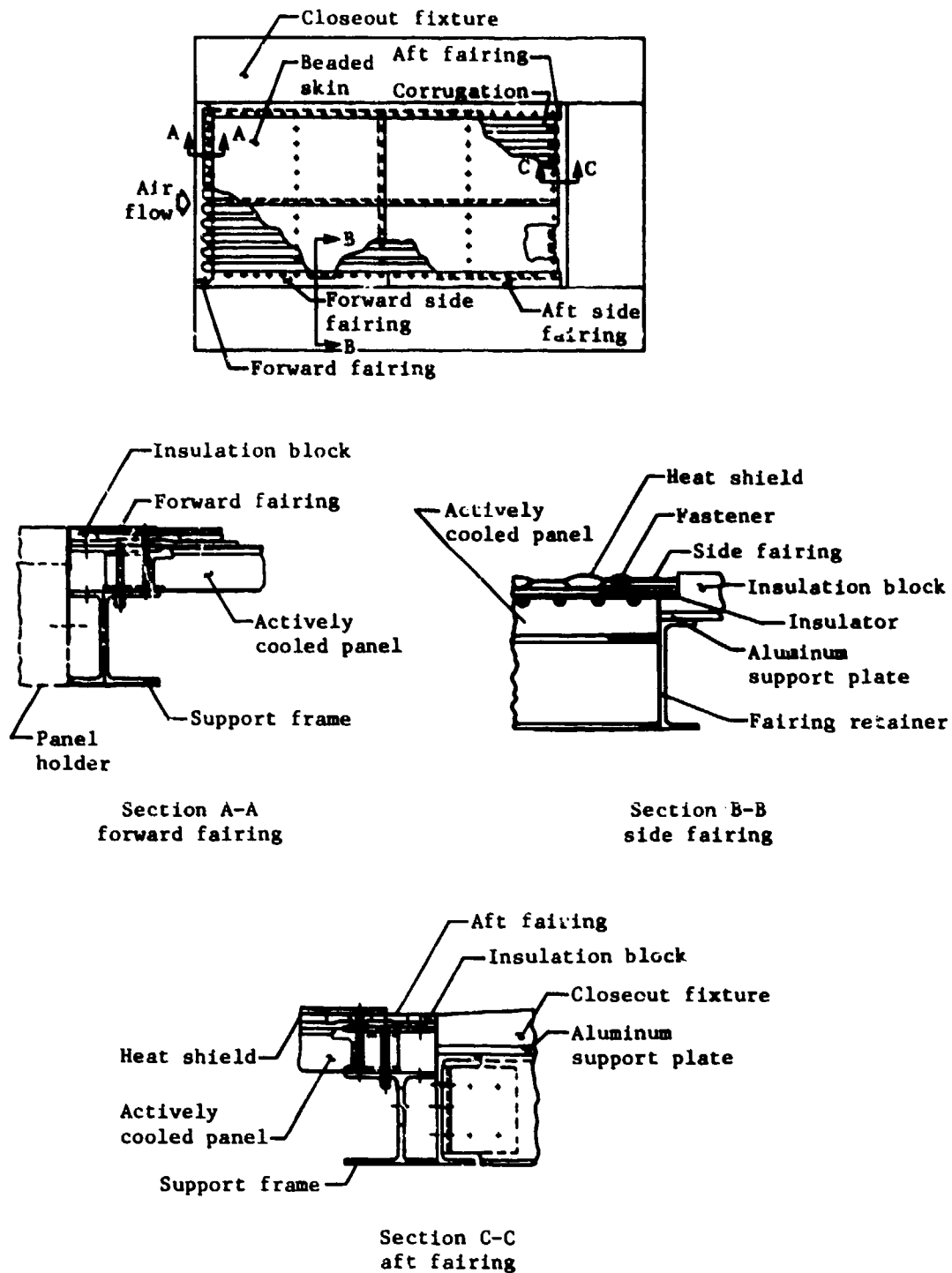
Figure 7.- Details of wind-tunnel closeout fixture.
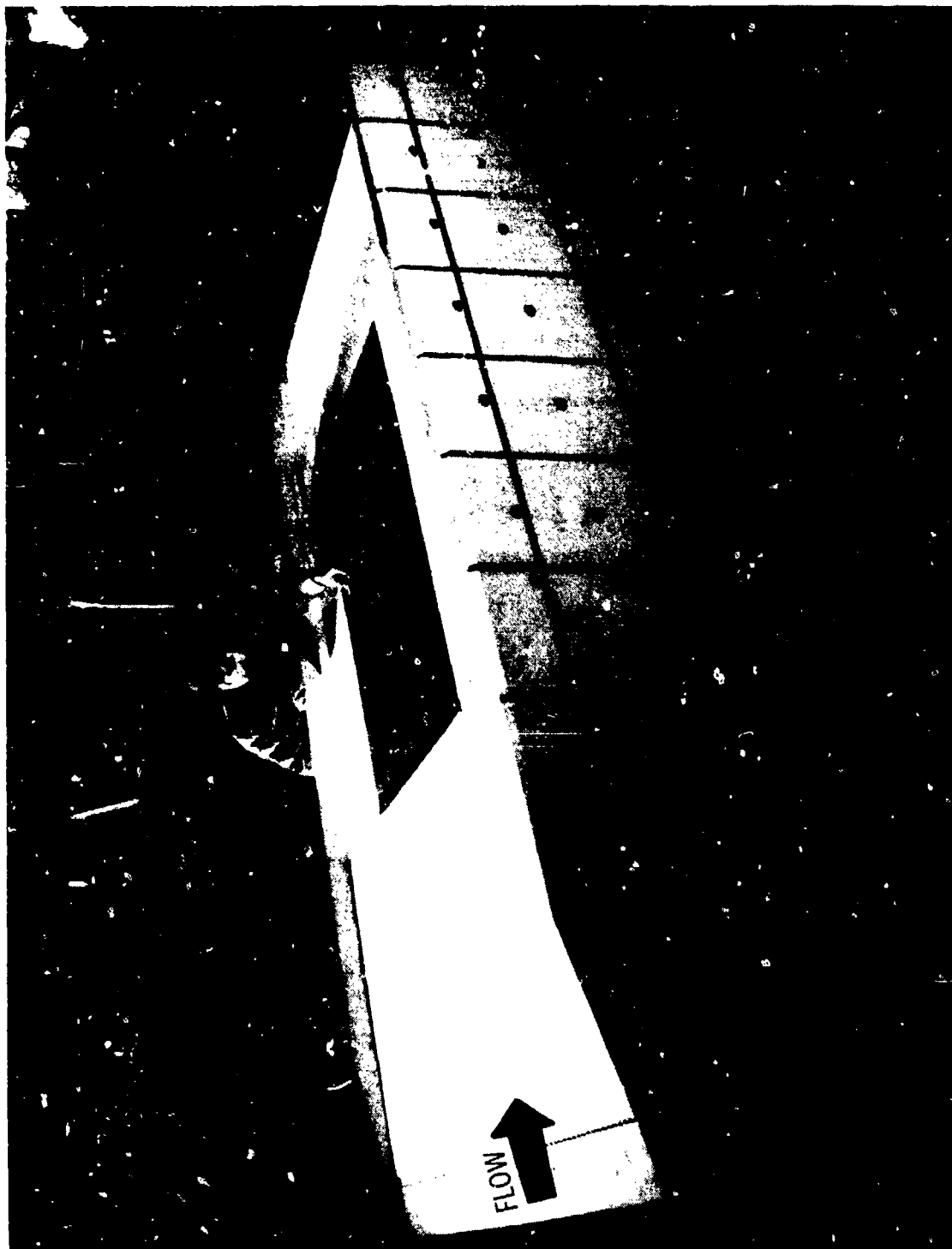
Figure 8.- RACP mounted in wind-tunnel test fixture.
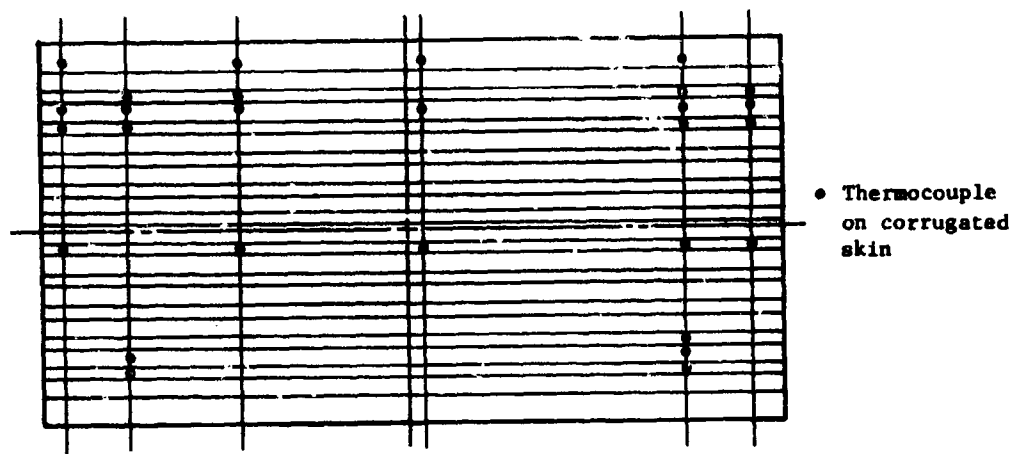
(a) Heat shields.
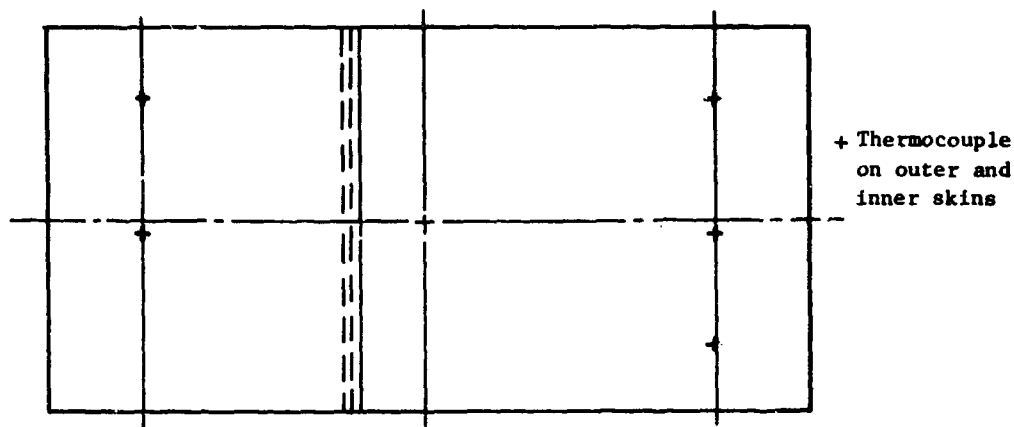
(b) Insulation packages.
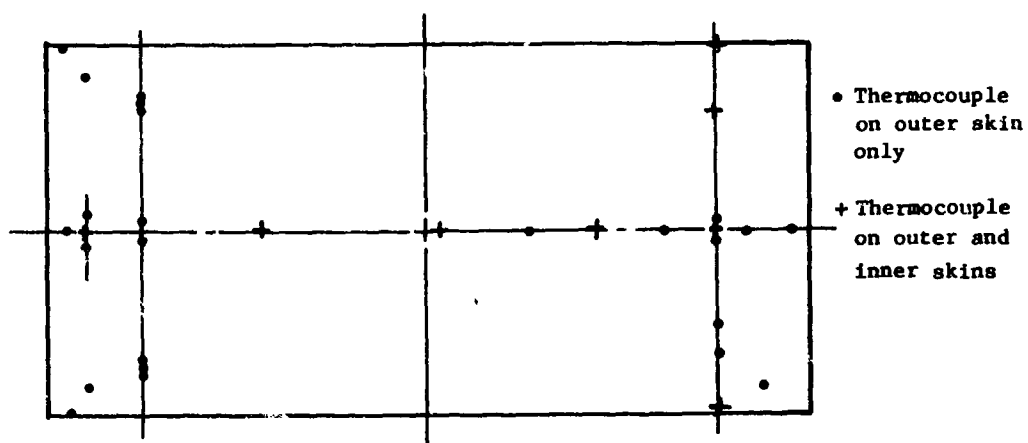
(c) Cooled panel.

Figure 9.- RACP thermocouple layout.
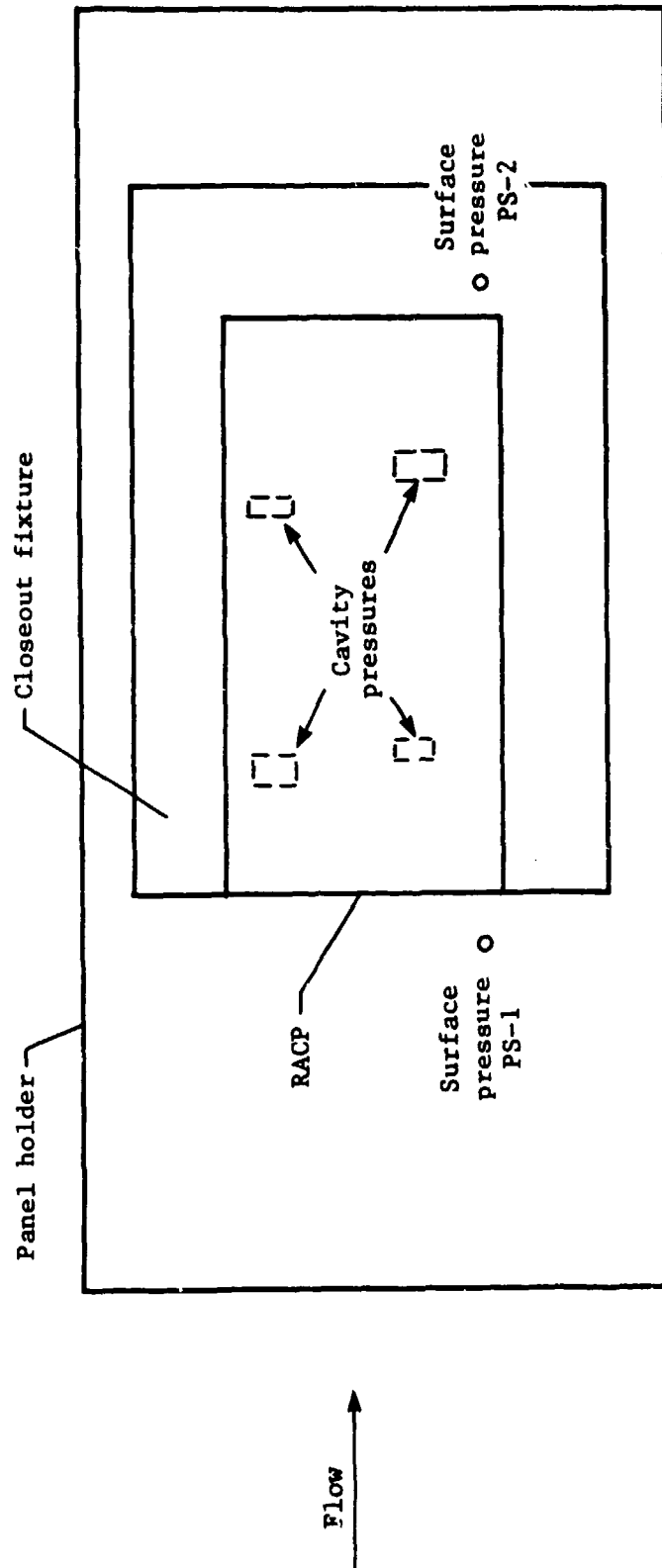
Figure 10.- Instrumentation location for surface and cavity measurements.

Flow

Test panel

Infrared camera with 25° lens

Infrared field of view

(a) Top view.

Infrared camera with 25° lens

Pressurized container

Pressurized container

High-speed camera

208 (82)

97 (38)

(b) Side view.
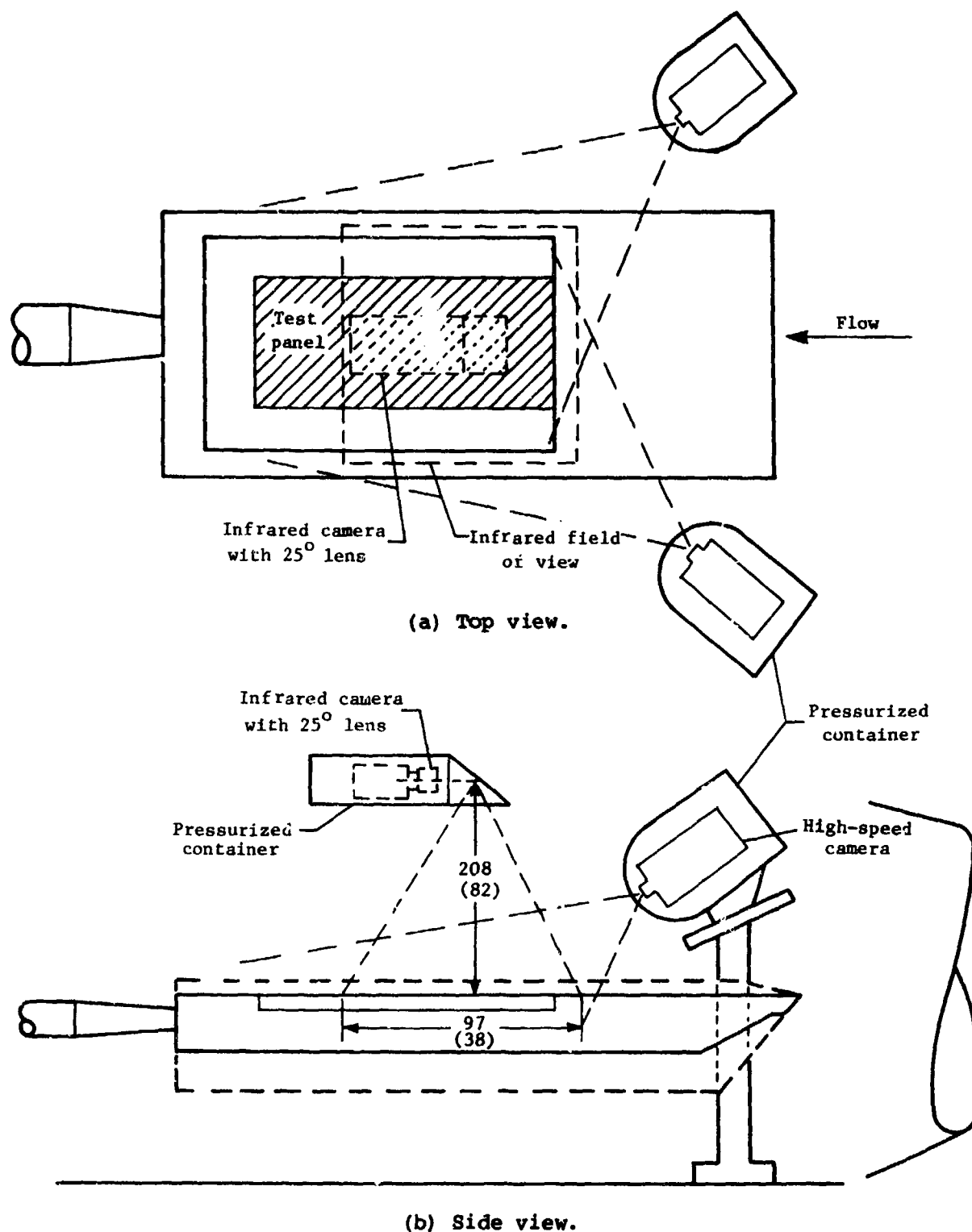
Figure 11.- Camera locations and view angles. (Dimensions are in cm (in.).)

(a) Schematic of tunnel.

(b) Model position during preheat.

(c) Model position during test.
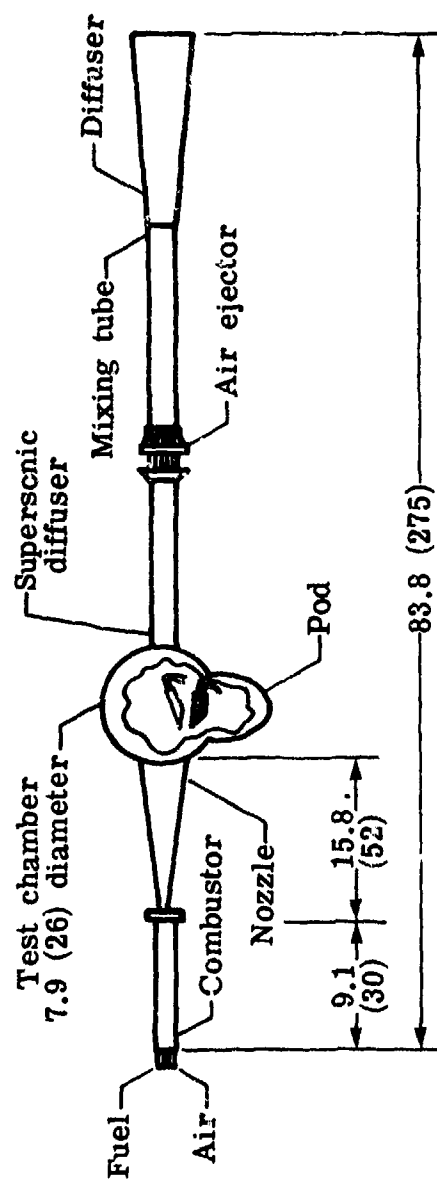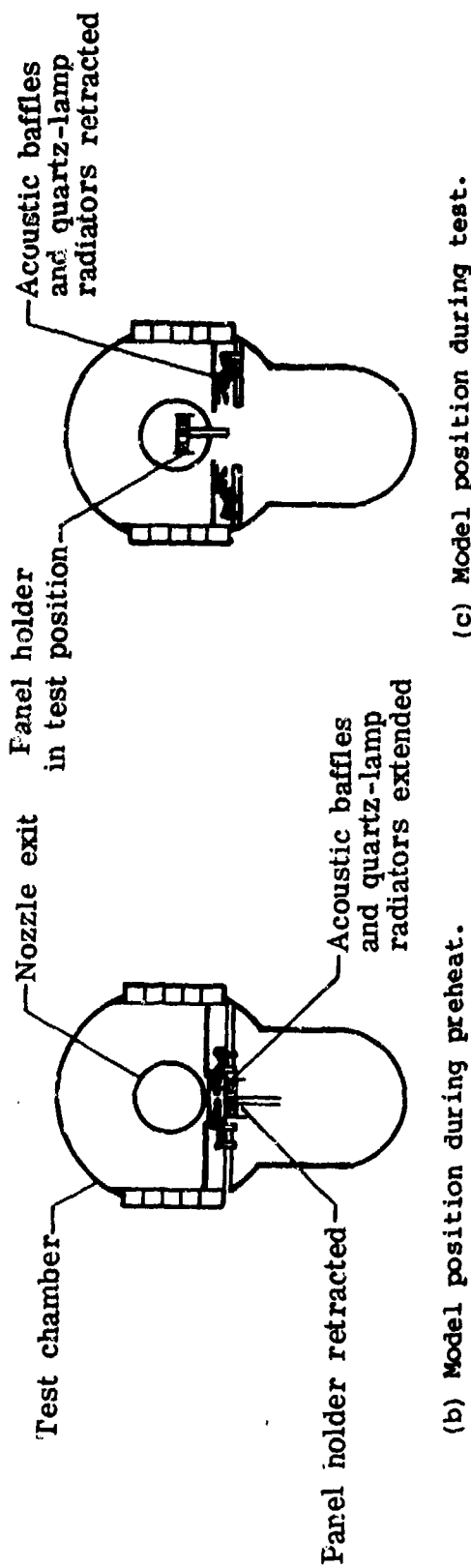
Figure 12.- Langley 8-foot high-temperature structures tunnel. (Dimensions are in m (ft).)
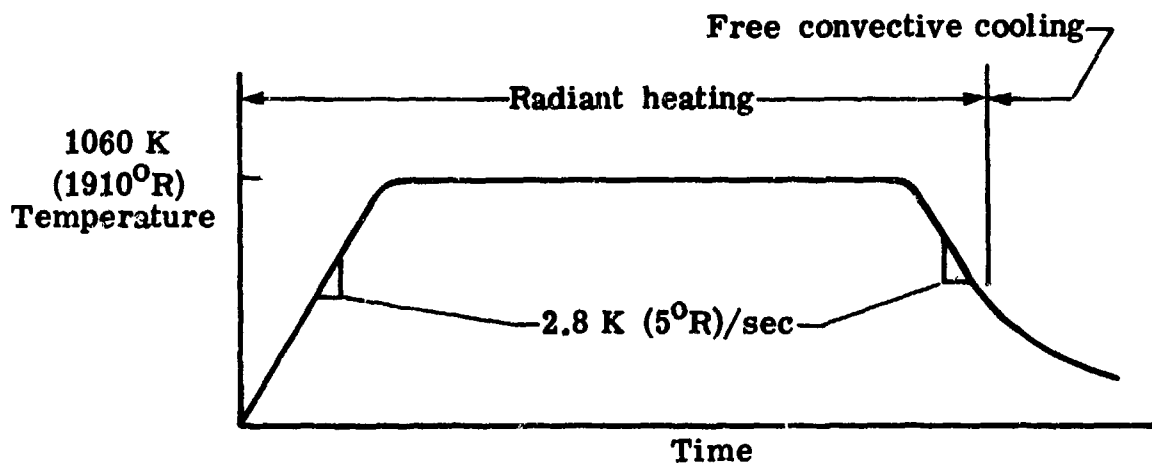
(a) Thermal cycle by radiant heating.
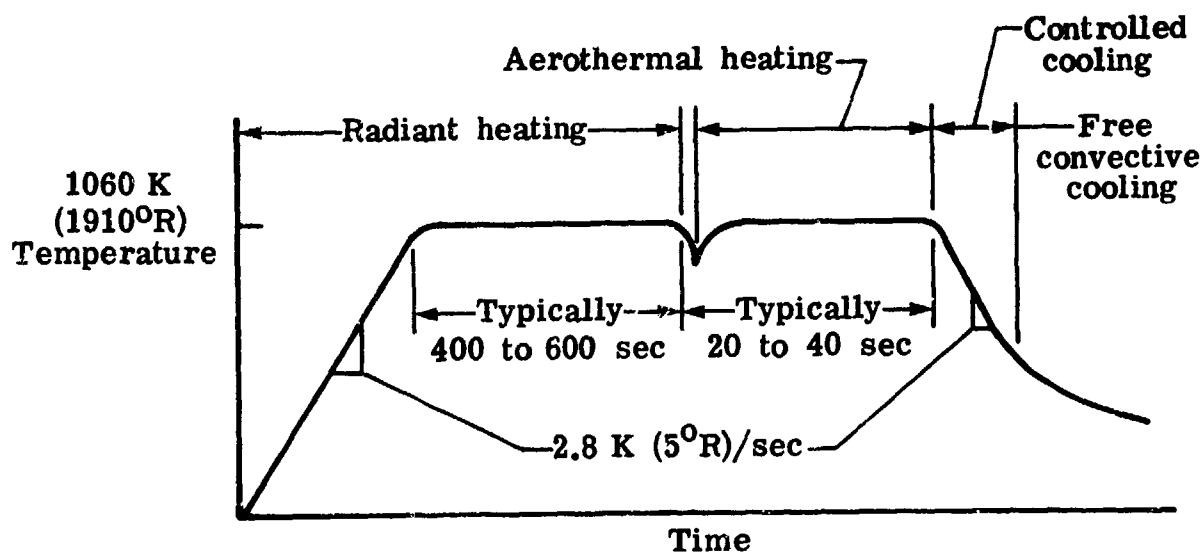
(b) Radiant-preheat aerothermal exposure.

Figure 13.- Typical surface temperature histories.
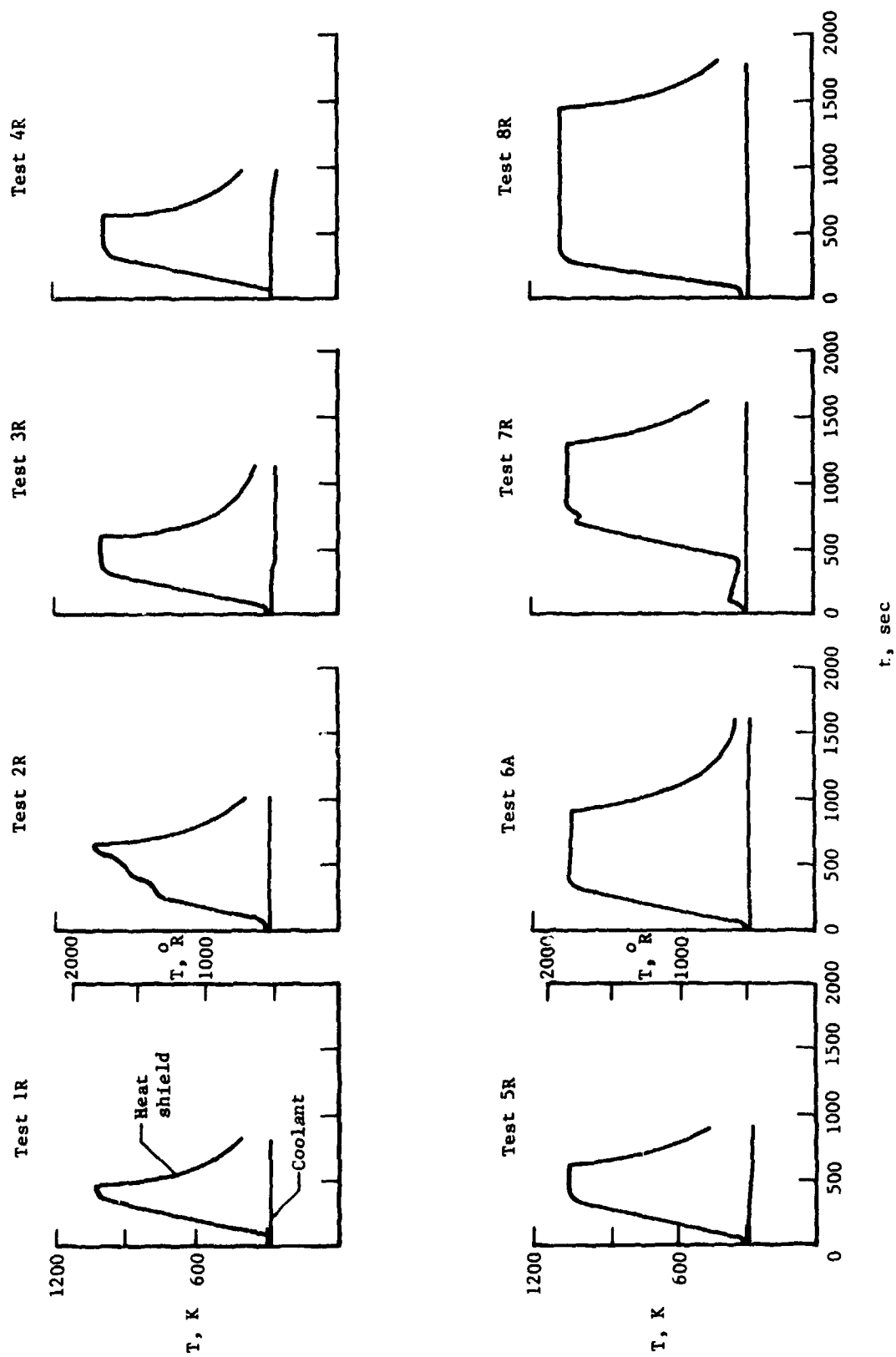
Figure 14.- Heat-shield and coolant inlet temperature histories. (R corresponds to radiant tests; A to aerothermal tests.)

31
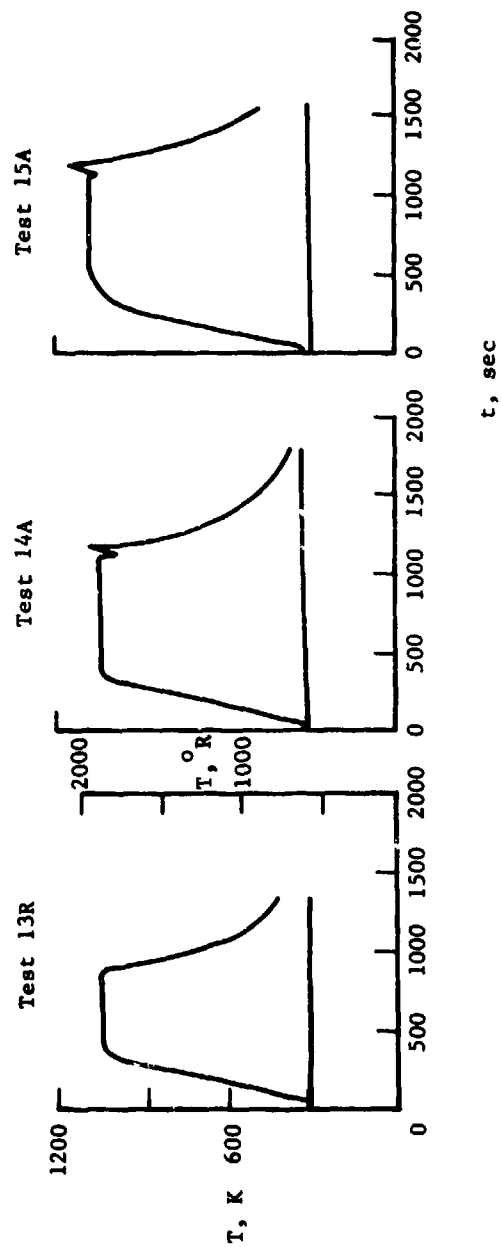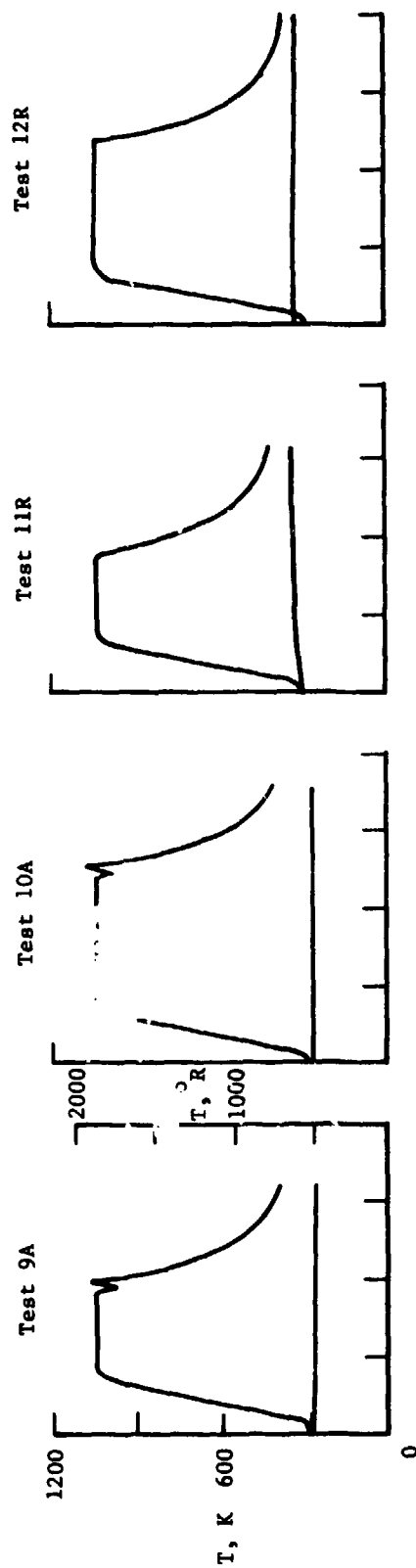
Figure 14.- Concluded.
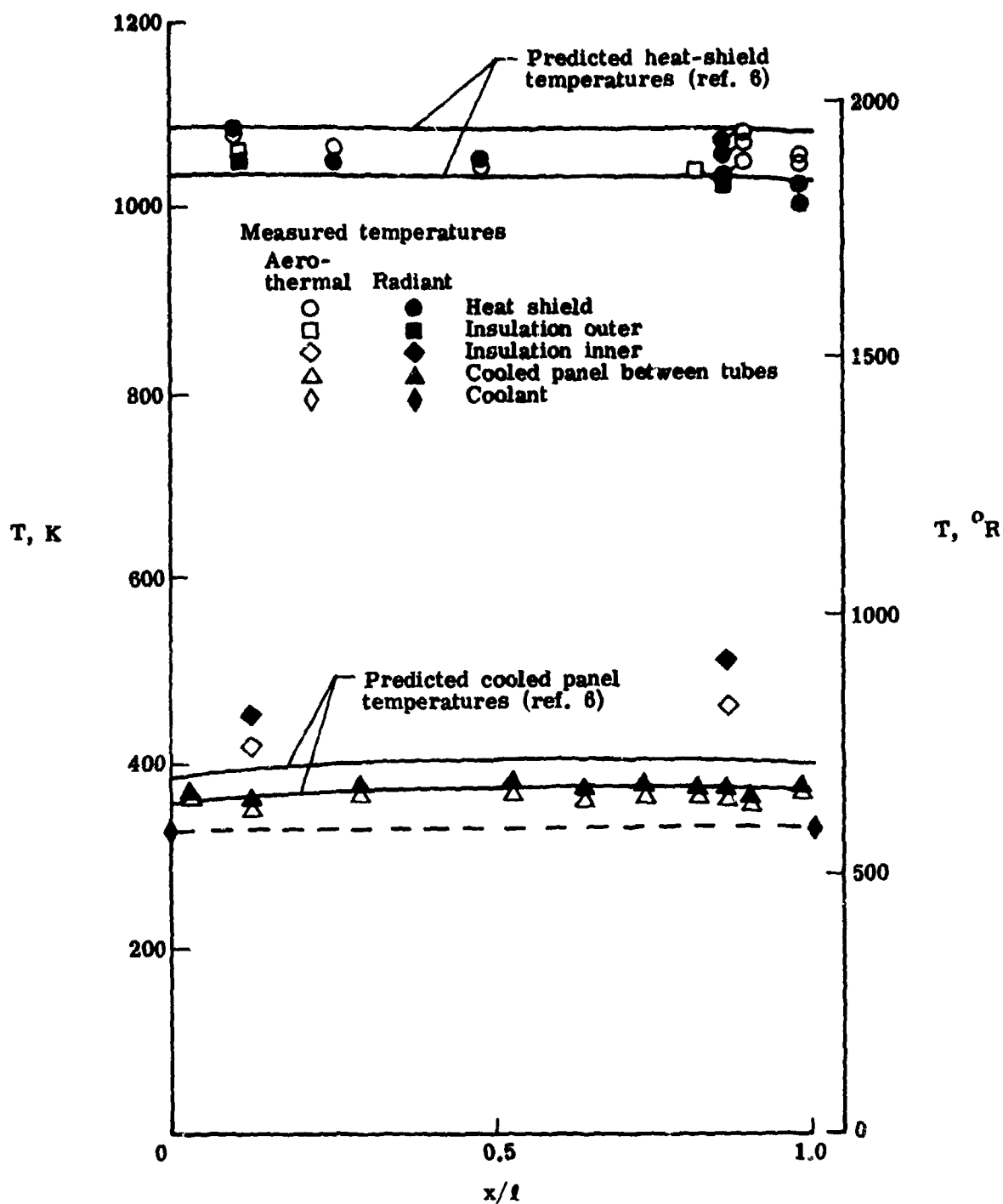
Figure 15.- Comparison of longitudinal temperature distributions from aerothermal and radiant heating for RACP (test 14).
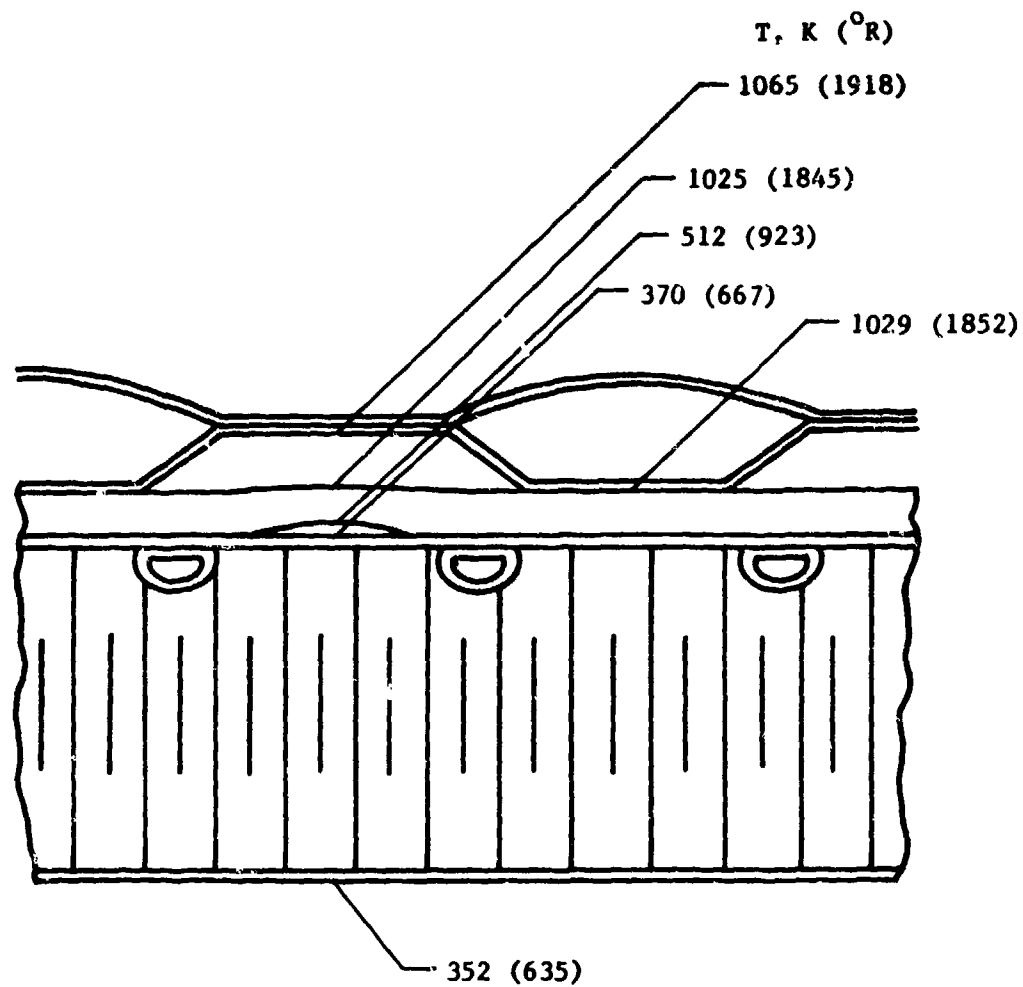
Figure 16.- Typical temperatures through radiative and actively cooled panel near panel exit (test 14 radiant preheat).

34
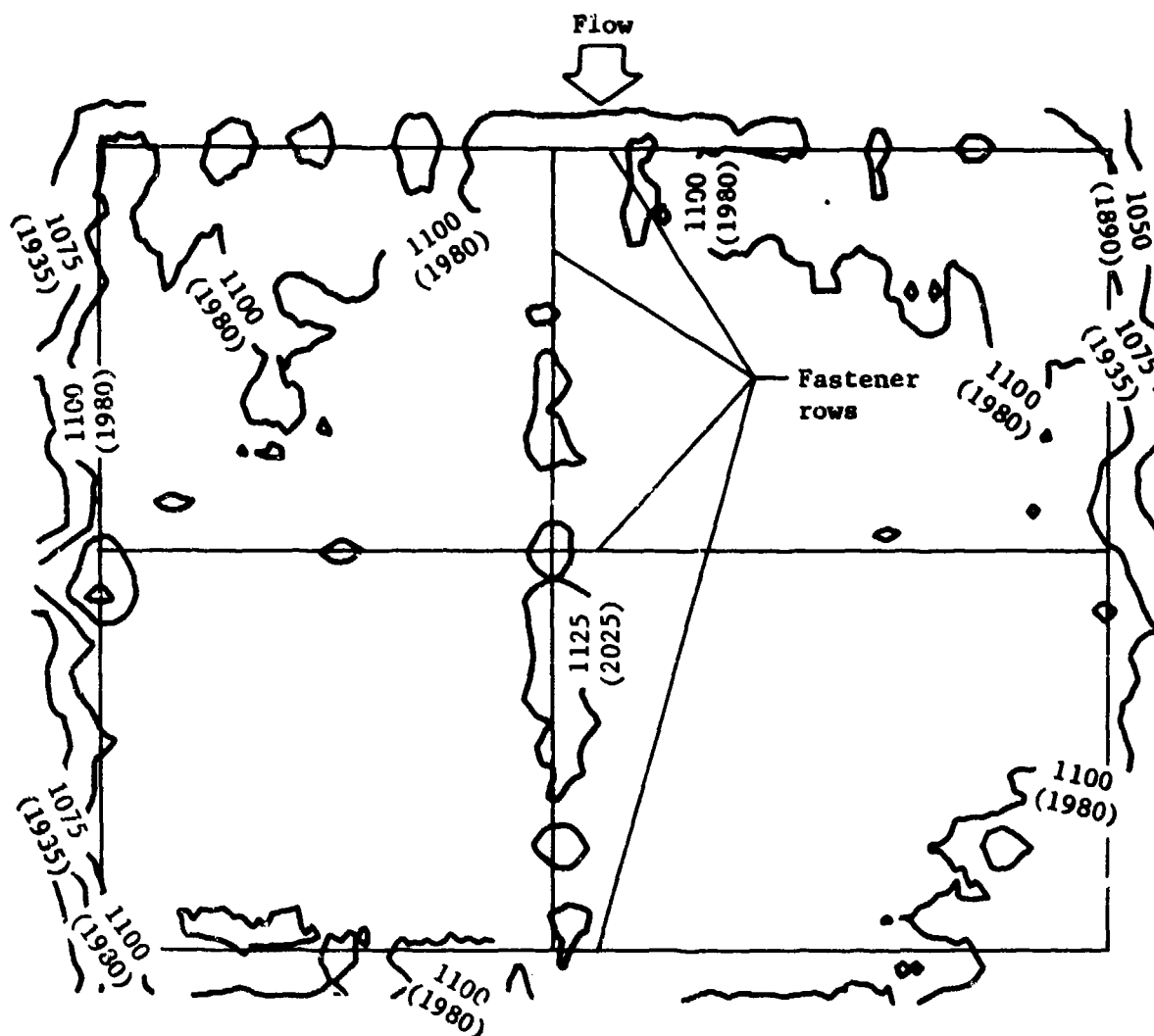
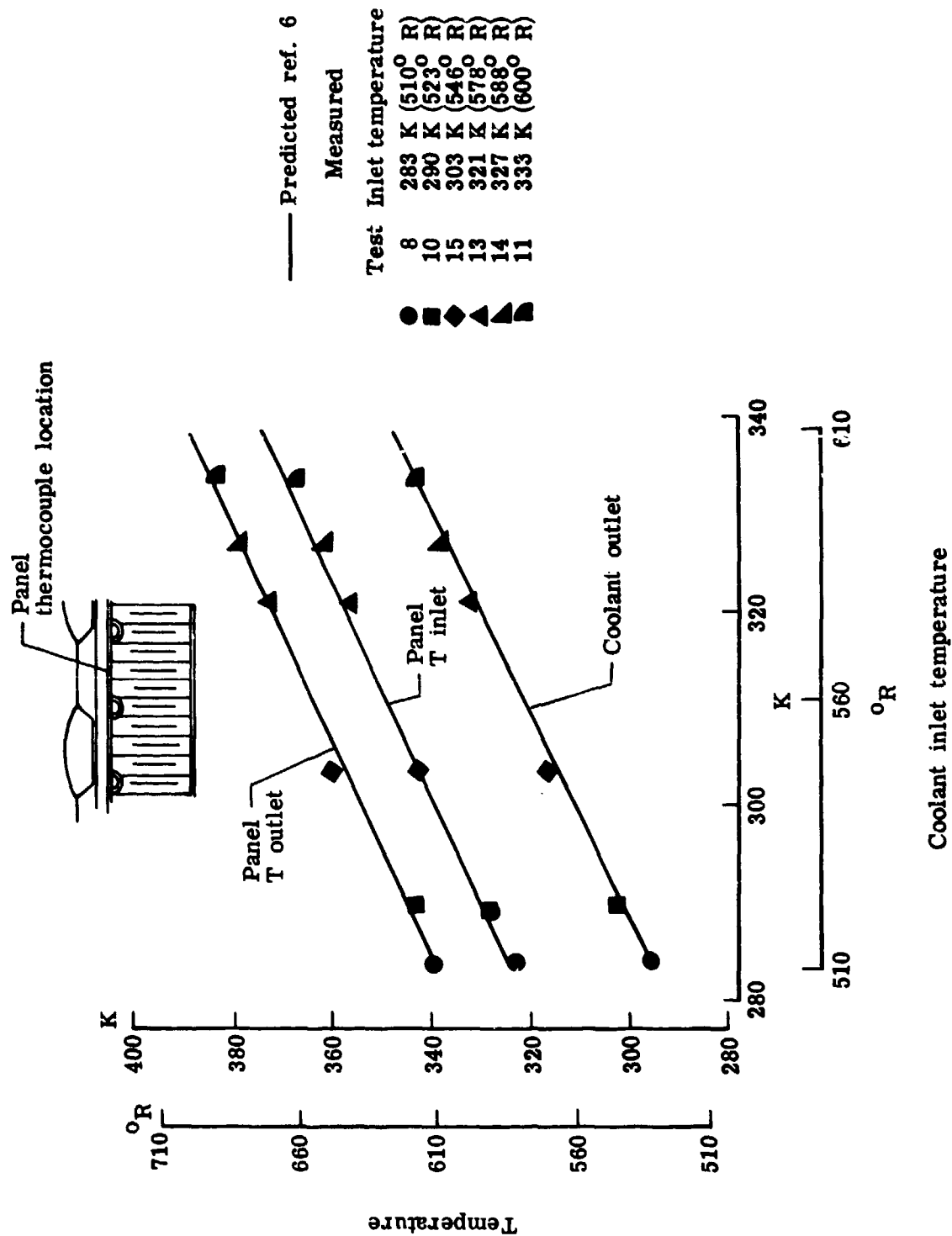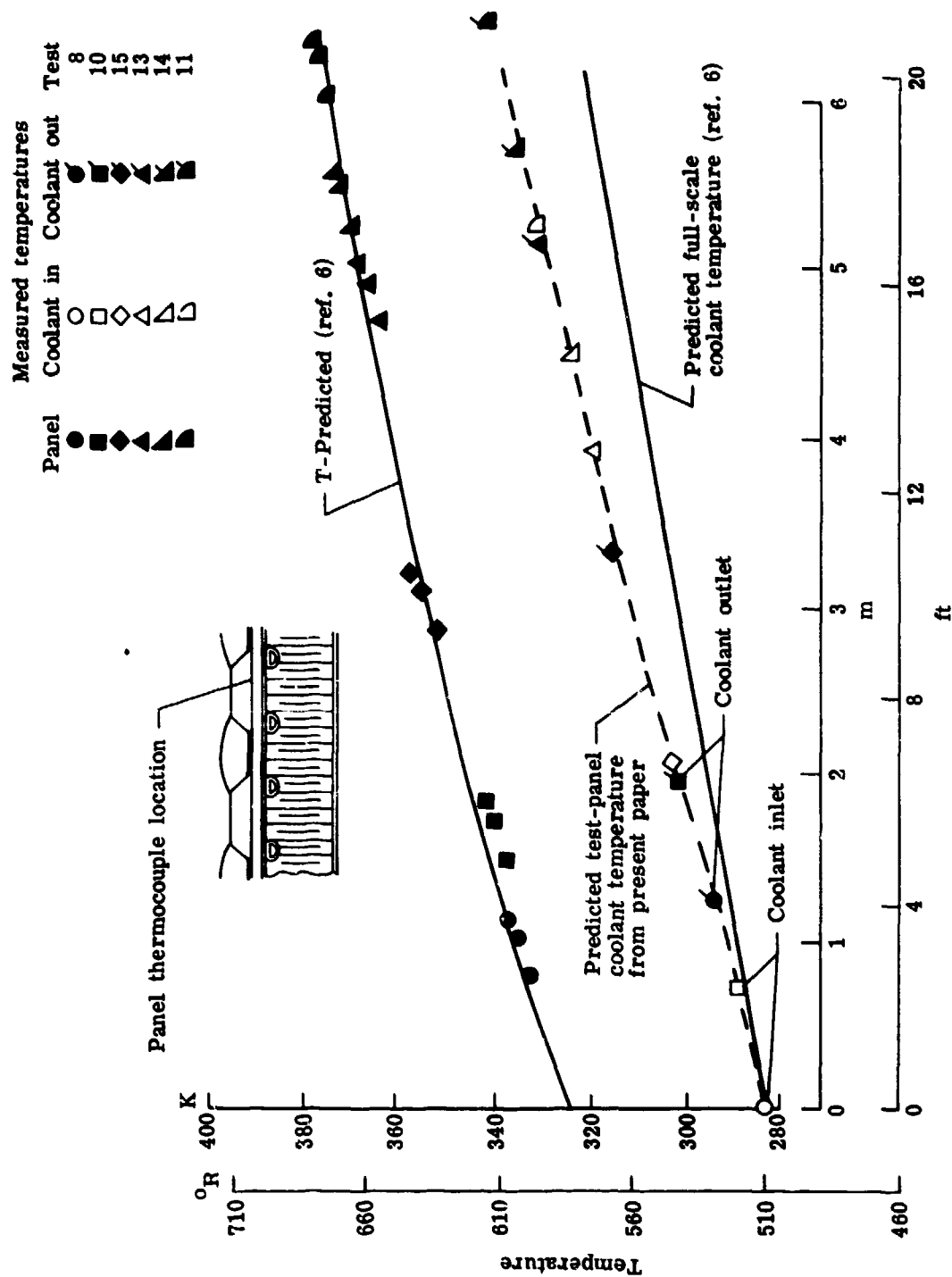Figure 17.- Heat-shield temperature contours, K (°R), from test 15.

Figure 18.- Comparison of measured and predicted cooled-panel temperatures as function of coolant inlet temperatures.

Figure 19.- Comparison of predicted and simulated full-scale (0.61 m (2 ft) by 6.1 m (20 ft)) cooled panel temperatures for RACP.

0.6-cm (0.25 in.) movement
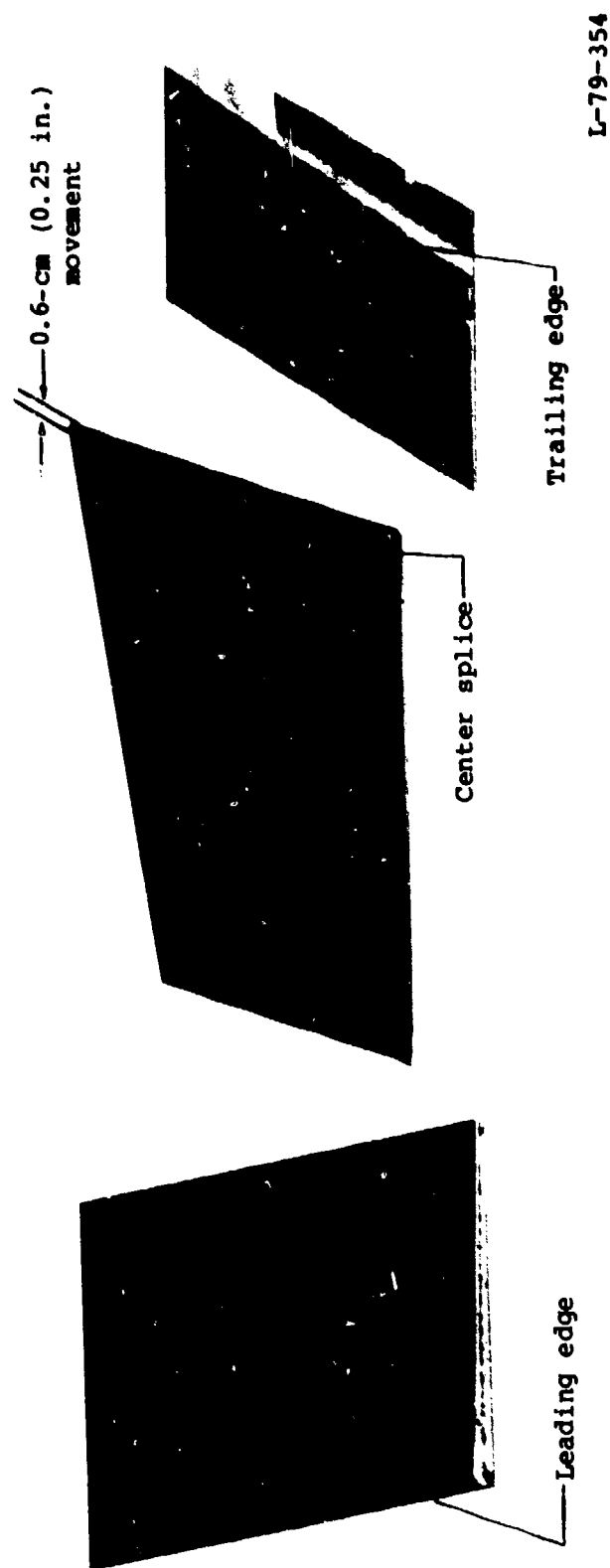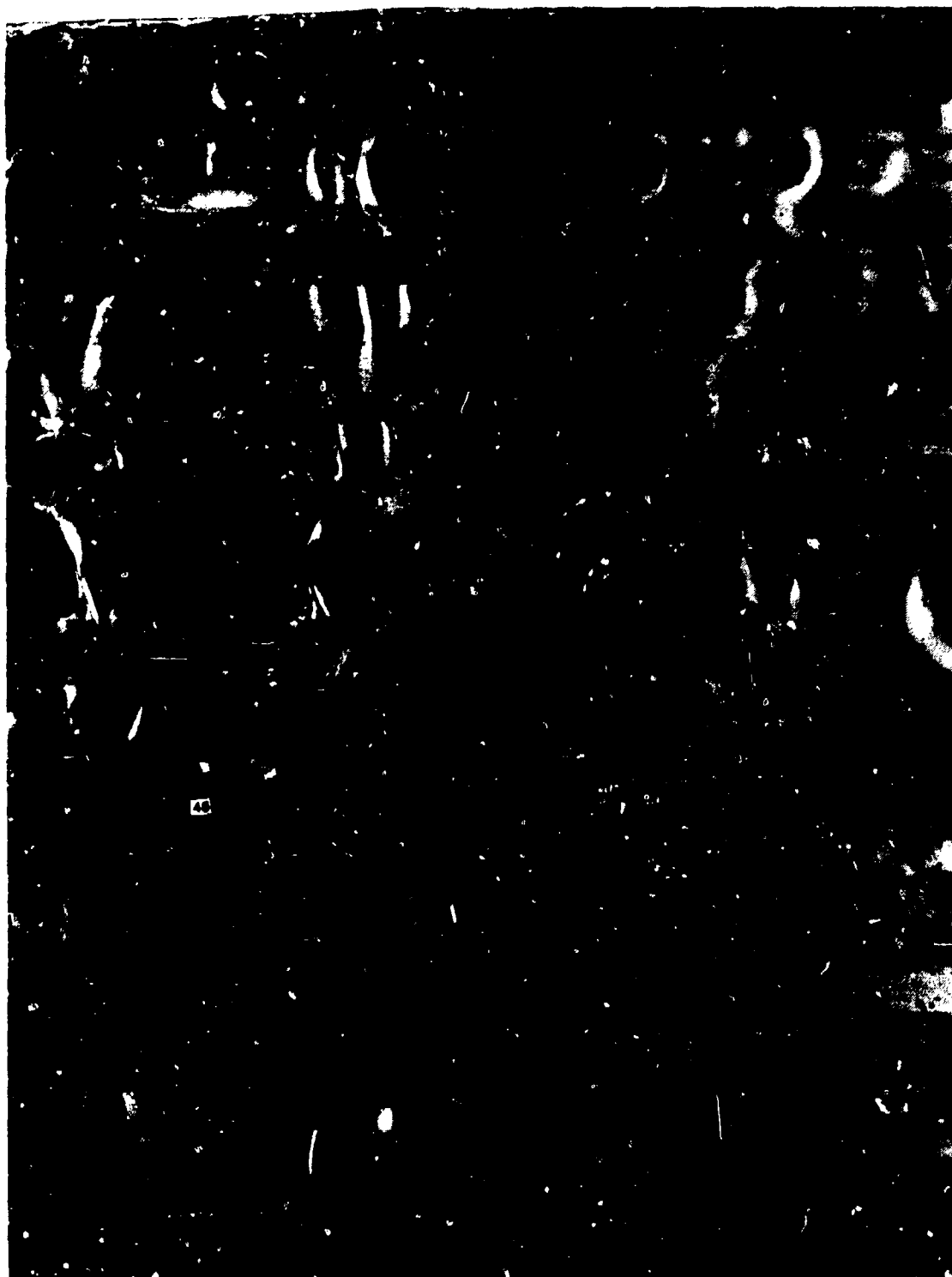
Center splice

Trailing edge

Leading edge

L-79-354

Figure 20.- Posttest condition of RACP heat shields.

Figure 21.- Posttest condition of RACP insulation packages.

L-78-5450

39

1. Report No. NASA TP-1595	2. Government Accession No.	3. Recipient's Catalog No.
4. Title and Subtitle AEROTHERMAL PERFORMANCE OF A RADIATIVELY AND ACTIVELY COOLED PANEL AT MACH 6.6		5. Report Date December 1979
		6. Performing Organization Code
7. Author(s) Charles P. Shore and Irving Weinstein		8. Performing Organization Report No. L-13355
9. Performing Organization Name and Address NASA Langley Research Center Hampton, VA 23665		10. Work Unit No. 505-33-73-03
		11. Contract or Grant No.
12. Sponsoring Agency Name and Address National Aeronautics and Space Administration Washington, DC 20546		13. Type of Report and Period Covered Technical Paper
		14. Sponsoring Agency Code

15. Supplementary Notes

16. Abstract

A flight-weight radiative and actively cooled honeycomb sandwich panel (RACP) was subjected to multiple cycles of both radiant and aerothermal heating. The 0.61-m (2 ft) by 1.22-m (4 ft) test specimen incorporated essential features of a full-scale 0.61-m (2 ft) by 6.10-m (20 ft) RACP designed to withstand a heat flux of 136 kW/m^2 (12 Btu/ft^2-sec). The panel consisted of René 41 heat shields, a thin layer of high-temperature insulation, and an aluminum honeycomb sandwich panel with coolant tubes next to the sandwich skin. A 60/40 mass solution of ethylene glycol/water was used to cool the panel which successfully withstood a total of 3.5 hr of radiant heating and 137 sec exposure to an $M = 6.6$ test stream. Heat-shield temperatures reached 1089 K (1945° R), and cooled-panel temperatures reached 382 K (687° R) midway between coolant tubes. Simulation of the full-scale panel indicated that the full-scale RACP would perform as expected. The tests revealed no evidence of coolant leakage or hot-gas ingress which would seriously degrade the RACP performance.

17. Key Words (Suggested by Author(s)) Active cooling Hypersonic aircraft Heated structures	18. Distribution Statement Unclassified – Unlimited Subject Category 34		
19. Security Classif. (of this report) Unclassified	20. Security Classif. (of this page) Unclassified	21. No. of Pages 39	22. Price* $4.50